



Published in final edited form as:

Cell Microbiol. 2014 September ; 16(9): 1405–1424. doi:10.1111/cmi.12302.

The ability of an attaching and effacing pathogen to trigger localized actin assembly contributes to virulence by promoting mucosal attachment

Emily M. Mallick¹, John J. Garber^{2,3,4}, Vijay K. Vanguri⁵, Sowmya Balasubramanian⁶, Timothy Blood¹, Stacie Clark⁶, Didier Vingadassalom¹, Christopher Louissaint¹, Beth McCormick¹, Scott B. Snapper^{2,4,7,*}, and John M. Leong^{1,6,*}

¹Department of Microbiology and Physiological Systems, University of Massachusetts Medical School, 55 Lake Avenue North, Worcester, MA 01655, USA.

²Division of Gastroenterology/Nutrition & Center for Inflammatory Bowel Disease Treatment and Research, Children's Hospital Boston, Boston, MA 02114, USA.

³Gastrointestinal Unit, Massachusetts General Hospital, Harvard Medical School, Boston, MA 02114, USA.

⁴Department of Medicine, Harvard Medical School, Boston, MA 02115, USA.

⁵Department of Pathology, University of Massachusetts Medical School, Worcester, Massachusetts 01655, USA.

⁶Department of Molecular Biology and Microbiology, Tufts University School of Medicine, 136 Harrison Avenue, Boston, MA, 02111, USA.

⁷Division of Gastroenterology & Hepatology, Brigham & Women's Hospital, Boston, MA, 02115, USA.

Abstract

Enterohemorrhagic *Escherichia coli* (EHEC) adheres to intestinal epithelial cells, then stimulates the actin nucleation promoting factor N-WASP to induce localized actin assembly resulting in an actin “pedestal”, the function of which is poorly understood. EHEC also produces Shiga toxin (Stx), which penetrates the intestinal epithelium to cause a life-threatening renal and systemic disease. To assess the role of pedestal formation in colonization and disease, we utilized the murine pathogen *Citrobacter rodentium*, which also forms actin pedestals, and the genetically engineered *C. rodentium* (Φ stx_{2dact}), which additionally triggers Stx-mediated systemic disease. We found that an intestine-specific N-WASP-deficient (iNWKO) mouse suffered dramatically less colonization and disease than N-WASP-proficient littermate controls when infected with either strain. In addition, upon infection of wild type mice, mutants of *C. rodentium* or *C. rodentium* (Φ stx_{2dact}) that are specifically defective in pedestal formation demonstrated a

***Contact information:** co-corresponding authors John M. Leong, Department of Molecular Biology and Microbiology, Tufts University School of Medicine, 136 Harrison Avenue, Boston, MA, 02111, USA. Phone: (617) 636-0488. Fax: (617) 636-0337. john.leong@tufts.edu. Scott B. Snapper, Division of Gastroenterology/Nutrition & Center for Inflammatory Bowel Disease Treatment and Research, Children's Hospital Boston; Enders 676, 300 Longwood Avenue, Boston, MA, 02115, USA. Phone: (617) 919-4973. Fax: (617) 730-0498. Scott.Snapper@childrens.harvard.edu..

relatively modest defect in cecal colonization and fecal shedding, but a more severe defect in colonization of the colonic mucosa. The *C. rodentium* (Φ stx_{2dact}) pedestal-defective mutant did not cause renal disease and, after normalizing for fecal bacterial load, was associated with a 16-fold lower risk of lethality. These findings suggest that the ability of an attaching and effacing pathogen to promote localized actin assembly contributes to virulence by promoting mucosal attachment.

Keywords

Enterohemorrhagic *E. coli*; actin pedestal; Hemolytic Uremic Syndrome; Shiga toxin; *Citrobacter rodentium*

Introduction

Enterohemorrhagic *Escherichia coli* (EHEC), particularly serotype O157:H7, is an important food-borne pathogen responsible for outbreaks of human diarrheal disease (Kaper et al., 2004, Pennington, 2010). EHEC infection can present as hemorrhagic colitis, as well as a life-threatening systemic disease known as hemolytic uremic syndrome (HUS), characterized by hemolytic anemia, thrombocytopenia, and renal failure (Karmali et al., 2009, Tarr et al., 2005). HUS is the leading cause of renal failure in children (Scheiring et al., 2008).

Systemic disease resulting from EHEC infection requires production of a phage-encoded Shiga toxin (Stx) (Schmidt, 2001). Stx produced in the gut traverses the intestinal epithelium, enters the blood stream, and targets organs expressing the globotriaosylceramide Gb₃ receptor, including the vasculature, kidneys, and central nervous system (Obrig, 2010, Schuller, 2011), where it inhibits protein synthesis. Of Stx1 and Stx2, the two major serotypes of Stx, EHEC strains that produce only Stx2 are associated with a greater risk of HUS (Melton-Celsa et al., 2011, Croxson and Finlay, 2010).

A distinctive colonization feature of EHEC that it shares with enteropathogenic *E. coli*, a cause of infantile diarrhea in the developing world, and *Citrobacter rodentium*, a closely related murine pathogen that causes colonic hyperplasia, is the ability to form attaching and effacing (AE) lesions on the intestinal epithelium (Kaper et al., 2004, Schauer and Falkow, 1993a). AE lesions are characterized by the effacement of brush border microvilli, intimate attachment of bacteria to the host cell, and the formation of actin ‘pedestals’ beneath bound bacteria (Moon et al., 1983, Kaper et al., 2004). Upon animal infection with EHEC or *C. rodentium*, mucosally adhered bacteria and AE lesions have been observed in the cecum, an initial site of colonization of mice by *C. rodentium*, colon, and rectum (Nart et al., 2008, Schauer and Falkow, 1993a, Dean-Nystrom et al., 1999, Nagano et al., 2003, Wales et al., 2001, Wiles et al., 2004). The relationship between two central features of EHEC pathogenesis, i.e. AE lesion formation and Stx-mediated disease, is relatively unexplored.

AE lesion formation is dependent on a type III secretion system (T3SS) that translocates bacterial effectors into host cells (Garmendia et al., 2005, McDaniel et al., 1995). Tir (translocated intimin receptor) is essential for pedestal formation and localizes to and spans

the host cell plasma membrane. The extracellular domain of Tir binds to the bacterial outer membrane protein intimin (Kenny et al., 1997, de Grado et al., 1999, Hartland et al., 1999), which then induces Tir clustering and the formation of actin pedestals in a process dependent on the host cell protein N-WASP (reviewed in (Caron et al., 2006, Campellone, 2010, Hayward et al., 2006)). For *C. rodentium* and EPEC Tir, the region critical for pedestal induction includes a tyrosine residue (TirY471 in *C. rodentium*, TirY474 in EPEC; (Kenny, 1999, Gruenheid et al., 2001, Campellone et al., 2002)) that is phosphorylated by mammalian cell kinases (Phillips et al., 2004, Swimm et al., 2004), creating a docking site for the host cell adaptor protein Nck (Gruenheid et al., 2001, Campellone et al., 2002, Campellone et al., 2004a). Nck recruits N-WASP, which, when activated, interacts with the Arp 2/3 actin nucleating complex and strongly stimulates localized actin polymerization beneath adherent bacteria (Frankel and Phillips, 2008, Rohatgi et al., 2001, Rivera et al., 2004). Although EHEC strains produce Tir and intimin, canonical EHEC Tir lacks a Nck binding sequence and instead translocates into host cells an additional bacterial factor, EspF_U (aka TccP) (Garmendia et al., 2004, Campellone et al., 2004b) which independently binds N-WASP and drives actin assembly via a Nck-independent pathway (Campellone and Leong, 2005, Brady et al., 2007). Interestingly, these two distinct actin polymerization signaling pathways are not absolute: some EPEC and EHEC strains possess redundant mechanisms of actin polymerization (Whale et al., 2006, Ogura et al., 2007).

While intimin and Tir are required for efficient host cell binding and for colonization in animal models (Deng et al., 2003, Schauer and Falkow, 1993b, Ritchie et al., 2003, Tzipori et al., 1995, Marches et al., 2000, Donnenberg et al., 1993), a number of studies have found that the specific ability of Tir to trigger actin assembly is dispensable for colonization. For example, murine infection with a 'pedestal-defective' *C. rodentium* strain (i.e., one that cannot trigger efficient pedestal formation on cultured mammalian cells) was not significantly attenuated for intestinal colonization compared to infection by a pedestal-competent strain (Deng et al., 2003). Similarly, fecal shedding in calves and lambs was unaltered upon infection with an EHEC pedestal-defective mutant (Vlisidou et al., 2006), and colonization of human intestinal explants by EPEC Tir phosphorylation-deficient mutants was similar to that of wild type, pedestal-competent EPEC strains (Schuller et al., 2007a).

In contrast, several studies have suggested that the ability to trigger actin pedestals may promote colonization. For example, compared to wild type strains, an EHEC pedestal-defective strain displayed a mild colonization defect late in infection of infant rabbits and generated smaller bacterial aggregates on the intestinal mucosa of gnotobiotic piglets (Ritchie et al., 2008). In addition, although a *C. rodentium* pedestal-defective mutant did not show a significant colonization defect during single infection, this strain was outcompeted by wild type *C. rodentium* during co-infection (Crepin et al., 2010).

Investigation of the role of AE lesion formation in systemic disease by EHEC has been limited by the lack of model systems that prominently manifest Stx-mediated systemic disease. We recently described a murine infection model utilizing a *C. rodentium* strain lysogenized with the Stx-producing phage Φ 1720a-02 (herein referred to as "*C. rodentium* (Φ stx2_{dact})"), that induces AE lesion formation, intestinal damage and renal compromise,

similar to EHEC toxin-mediated disease (Mallick et al., 2012b). We infected a murine host defective in pedestal formation with either non-toxigenic *C. rodentium* or *C. rodentium* ($\Phi stx2_{dact}$), and a wild type murine host with mutants of *C. rodentium* or *C. rodentium* ($\Phi stx2_{dact}$) that are incapable of robust pedestal formation. Our results revealed that the ability of the AE pathogen to trigger localized actin assembly contributes to virulence by promoting mucosal attachment, particularly in the colon.

Results

Mice devoid of intestinal N-WASP do not permit AE pathogen-induced pedestal formation or mucosal colonization

To determine the requirement for pedestal formation for colonization by AE pathogens, we generated mice deficient in N-WASP, a host protein required for AE pathogen-induced actin pedestal assembly. Since germline deletion of N-WASP results in early embryonic lethality (Snapper et al., 2001, Lommel et al., 2001), we generated mice specifically devoid only of intestinal N-WASP (i.e., iNWKO mice). Western blot analysis confirmed that N-WASP was expressed in the colon, ileum, and jejunum of littermate control mice (designated “LMC” in figures), but was absent from these sites in iNWKO mice (Fig. 1A). iNWKO mice were viable but gained weight less rapidly than their littermate controls (Fig. 1B, C), specifically between eight and 15 weeks of age (Fig. 1C). Histologic examination of intestinal tissue from iNWKO mice revealed grossly normal crypt-villous architecture and the presence of all epithelial cell lineages, (Sup. Fig. 1). Although iNWKO mice displayed abnormal microvilli and decreased perijunctional actin, there was no evidence of spontaneous inflammation, neutrophilic infiltrate, or increased cellularity of the lamina propria (Sup. Fig. 1).

To determine if colonization was dependent on intestinal N-WASP, iNWKO and littermate control mice were infected for seven days with approximately 5×10^8 CFU of GFP-*C. rodentium* (see Sup. Table 1). Despite repeated attempts, mucosal colonization of the colons of iNWKO mice, in contrast to littermate controls, was insufficient to permit reliable assessment AE lesions by transmission electron microscopy (TEM) (data not shown). Therefore, we evaluated colonic mucosal-association of *C. rodentium* using immunofluorescent (IF) analyses. Whereas the colonic mucosa of infected littermate controls revealed large numbers of bound bacteria, no mucosal-associated bacteria were detected in the colons of infected iNWKO mice (Fig. 2A-B).

To further evaluate colonization by *C. rodentium* in the absence of N-WASP, fecal shedding was assessed in iNWKO and littermate control mice by quantifying bacterial CFU/g stool. Fecal shedding in iNWKO mice was ~100-fold lower than in littermate control mice at seven days post-infection (Fig. 2C). In contrast, oral infection of iNWKO mice by another intestinal pathogen, *Salmonella enterica*, resulted in intestinal colonization with concomitant inflammatory changes in the mucosa indistinguishable from that of littermate controls (Sup. Fig. 2A, D, and E). Together, these data indicate that N-WASP is required for intestinal colonization by *C. rodentium*.

N-WASP promotes high-level colonization and systemic disease during toxigenic *C. rodentium* infection

To determine whether the N-WASP pathway of actin pedestal formation was required for high-level fecal shedding upon infection with toxigenic *C. rodentium*, iNWKO and littermate control mice were infected with approximately 1×10^9 CFU *C. rodentium* (Φ stx₂dact) by oral gavage. Viable stool counts throughout infection showed that fecal shedding in littermate controls reached a peak of approximately 10^9 CFU/g stool between 11 and 14 days post-infection and slowly diminished thereafter (Fig. 3A and Sup. Fig. 3A). By 30 days post-infection, bacteria were no longer detected in the stool, as previously observed in immunocompetent mice (Sup. Fig. 3A; (Vallance et al., 2002, Simmons et al., 2003, Ghaem-Maghani et al., 2001)). In contrast, average peak fecal shedding of *C. rodentium* (Φ stx₂dact) by iNWKO mice was dramatically diminished (Fig. 3A) and bacteria were absent in stool by 30 days post-infection (Sup. Fig. 3A).

Weight loss is common in murine models of HUS (Mallick et al., 2012b, Mohawk and O'Brien, 2011). N-WASP-proficient littermate controls infected with *C. rodentium* (Φ stx₂dact) maintained body weight through nine days post-infection, but lost significant weight, averaging 15.5%, thereafter (Fig. 3B and Sup. Fig. 3B). Maximal weight loss typically occurred at peak colonization or just prior to euthanasia due to the deteriorating condition of the animals (Fig. 3B). Mice that did not succumb to lethal disease regained body weight as fecal counts diminished to zero by approximately 25 days post-infection (Sup. Fig. 3B). In contrast, body weight of iNWKO mice remained constant throughout the course of infection (Fig. 3B and Sup. Fig. 3B).

As intestinal damage is often observed in patients with HUS and in murine infection by *C. rodentium* (Φ stx₂dact) (Mallick et al., 2012b), intestinal sections of iNWKO mice and littermate control mice infected with *C. rodentium* (Φ stx₂dact) were examined histologically. Littermate control intestines displayed severe damage to the mucosal surface, infiltration of inflammatory cells, crypt withering, and depletion of goblet cells (Fig. 3C), all evidence of acute injury. In contrast, the intestines of iNWKO mice appeared histologically normal.

Renal damage, a hallmark of Stx-mediated disease, was evaluated both histologically and functionally in iNWKO and littermate control mice infected with *C. rodentium* (Φ stx₂dact). N-WASP-proficient littermate control mice showed severe proximal tubular damage, with sloughed cells in the lumen and flattening of the epithelium (Fig. 3D). Mitotic activity was observed in some proximal tubule cells, presumably reflecting regeneration of damaged cells (V.V. and E.M. unpub. obs.). This renal pathology corresponded to functional compromise, as littermate control mice developed significant proteinuria, specifically early in infection and at time points corresponding to peak fecal shedding, i.e., at approximately ten days post-infection (Fig. 3E). In contrast, the kidneys of iNWKO mice showed no evidence of histological damage, and protein was not detected in the urine (Fig. 3D, E). The absence of systemic damage to iNWKO mice infected with *C. rodentium* (Φ stx₂dact) was specific to that enteric pathogen, as *Salmonella*-infected iNWKO mice suffered hepatic and splenic colonization and damage indistinguishable from littermate controls (Sup. Fig. 2B, C, and E).

The absence of weight loss, intestinal damage, and kidney dysfunction in infected iNWKO mice corresponded to 100% survival (Fig. 3F). In contrast, approximately 35% of littermate control mice infected with *C. rodentium* (Φ stx_{2dact}) succumbed to lethal disease (Fig. 3F). These data indicate that N-WASP, a host factor critical for pedestal formation, is required for Stx-mediated weight loss, intestinal and renal damage, and lethality after infection with *C. rodentium* (Φ stx_{2dact}).

***C. rodentium* Tir-mediated actin assembly promotes colonization of the colonic mucosa**

Mice specifically deficient for intestinal N-WASP displayed changes in microvillar architecture and junctional integrity (data not shown) that could contribute in unpredictable ways to differences in responses to *C. rodentium* infection. In addition, N-WASP has been shown to increase effector translocation (Vingadassalom et al., 2010) a process necessary for efficient colonization (Ritchie and Waldor, 2005, Deng et al., 2004), so the colonization defect observed in the iNWKO mice may partially be due to diminished type III translocation. Therefore, we also examined the role of pedestal formation in intestinal colonization by utilizing a bacterial *tir* point mutant defective for pedestal formation. We generated plasmid, pTirY471F, encoding *C. rodentium* TirY471F that, despite promoting attachment to cultured cells, does not promote pedestal formation *in vitro* because of the lack of the tyrosine residue critical for Nck recruitment (Deng et al., 2003, Crepin et al., 2010). An equivalent tyrosine to phenylalanine substitution in EPEC Tir gave rise to a similar phenotype in EPEC (Schuller et al., 2007a). Western blot analysis of bacterial pellets and culture supernatants revealed that *C. rodentium tir* (Mallick et al., 2012a) harboring pTirY471F produced and secreted levels of Tir indistinguishable from an isogenic strain harboring pTir_{WT} (Mallick et al., 2012b) (Sup. Fig. 4A, B).

As previously shown (Deng et al., 2003, Mallick et al., 2012b, Crepin et al., 2010), whereas mice infected with wild type *C. rodentium* shed high levels of bacteria in the feces (Fig. 4A), those infected with *C. rodentium tir* displayed fecal counts below the limit of detection (<100 CFU/g feces; data not shown). pTir_{WT} significantly, but partially, complemented the fecal shedding defect of *C. rodentium tir*, with slightly delayed kinetics (Fig. 4A), similar to complementation by plasmid-encoded Tir in other studies (Deng et al., 2003, Mallick et al., 2012b). Consistent with partial complementation by pTir, TEM of the colonic mucosa revealed very few bound *C. rodentium tir*/pTir_{WT} (data not shown), although IF staining, which samples larger areas, readily revealed bound bacteria (see below). Approximately a third of recovered fecal bacteria lost the Tir-encoding plasmid (Sup. Table 4), likely contributing to the partial nature of the complementation. pTirY471F also partially complemented *C. rodentium tir* for fecal shedding, although to a somewhat lesser degree than pTir_{WT} (Fig. 4A). An analysis of multiple experiments confirmed that peak fecal shedding (i.e. the single-highest titer of fecal CFU observed during the course of infection) by mice infected with *C. rodentium tir*/pTirY471F was approximately three-fold lower than by mice infected with *C. rodentium tir*/pTir_{WT} (p=0.0121; Fig. 4B, Table 1). This result could not be attributed to a differential loss of pTir_{WT} and pTirY471F, as both plasmids were retained by *C. rodentium tir* to the same degree throughout infection (Sup. Table 4).

C. rodentium initiates infection in the murine cecum, then spreads to the colon after several days (Wiles et al., 2004). To determine if actin pedestal formation is particularly important to colonization of a specific intestinal segment, mice infected with either *C. rodentium* *tir*/pTir_{WT} or *C. rodentium* *tir*/pTirY471F were euthanized and necropsied at the approximate peak of fecal shedding (i.e. six days post-infection). We quantitated bacteria in luminal washings, as well as cecum- or colon-associated bacteria retained after removal of feces and luminal washings. In luminal washings, *C. rodentium* *tir*/pTirY471F was present at ~three-fold lower levels than *C. rodentium* *tir*/pTir_{WT}, similar to the ~four-fold lower levels of *C. rodentium* *tir*/pTirY471F found in feces (Fig. 4C, **first and second panels**). Similarly, *C. rodentium* *tir*/pTirY471F was present in cecal homogenates at ~six-fold lower levels than bacteria producing *C. rodentium* *tir*/pTir_{WT} (Fig. 4C, **third panel**). None of the above differences in bacterial counts reached statistical significance. However, in contrast, *C. rodentium* *tir*/pTirY471F displayed a significant ~16-fold reduction in colonic colonization compared with *C. rodentium* *tir*/pTir_{WT} (Fig. 4C, **fourth panel**).

We next used IF staining to localize the association of pedestal-competent (*C. rodentium* *tir*/pTir_{WT}) and pedestal-defective (*C. rodentium* *tir*/pTirY471F) bacteria with the mucosal surfaces of the cecum and colon during infection near peak fecal shedding (when the fecal concentrations of the two bacterial strains were similar). Randomly chosen cecal samples from each infected mouse were visually scored (**Materials and Methods**), revealing that 53% of mice (9/17) infected with *C. rodentium* *tir*/pTir_{WT} were positive for mucosal attachment, whereas 12% of cecal specimens (2/17) from mice infected with *C. rodentium* *tir*/pTirY471F were positive ($0 < 0.01$; Fig. 4D; Table 2). These results were consistent with our finding that cecal homogenates contained ~six-fold fewer *C. rodentium* *tir*/pTirY471F CFU than *C. rodentium* *tir*/pTir_{WT} (Fig. 4C). In the colon, none of the 17 mice infected with *C. rodentium* *tir*/pTirY471F displayed mucosally attached bacteria (Fig. 4D), compared with 53% of mice (9/17) infected with the pedestal-competent strain ($p < 0.001$; Table 2), consistent with the more severe (~16-fold) colonic colonization defect seen with pedestal-defective *C. rodentium* (Fig. 4C).

Tir-mediated actin assembly by *C. rodentium* (Φ stx_{2dact}) promotes colonization of the colonic mucosa

Stx is essential for systemic disease (Mallick et al., 2012b, Mohawk and O'Brien, 2011) and, additionally, promotes EHEC colonization in a murine model (Robinson et al., 2006). We previously noted that *C. rodentium* (Φ stx_{2dact}) exhibited an approximately three- to ten-fold enhancement of fecal shedding compared with the non-lysogenic *C. rodentium* parental strain, but this difference did not reach statistical significance using experimental groups of five mice (Mallick et al., 2012b). We therefore pooled multiple experiments encompassing many (i.e. >250) mice and found that peak fecal shedding of *C. rodentium* (Φ stx_{2dact}) was approximately six-fold higher ($p < 0.0001$) than that of the parental non-lysogenic *C. rodentium* strain (Table 1). Lysogeny by Φ stx_{2dact} did not appear to alter the kinetics of infection, as peak fecal shedding occurred at ~six to eight days post-infection for both strains (Mallick et al., 2012b).

We further found that *C. rodentium* (Φ stx_{2dact}) tir/pTir_{WT} and *C. rodentium* (Φ stx_{2dact}) tir/pTirY471F produced and secreted similar levels of Tir (Sup. Fig. 4C, D) and bound indistinguishably to cultured murine cells. On average, each mammalian cell bound 6.89 ± 0.62 versus 6.50 ± 1.7 bacteria for pTir_{WT} and pTirY471F strains, respectively (Sup. Fig. 5A), despite the inability of *C. rodentium* (Φ stx_{2dact}) tir/pTirY471F to generate actin pedestals on cultured cells (Sup. Fig. 5B). Tir was clearly required for efficient binding, as mammalian cells bound an average of only 0.04 Tir-deficient bacteria.

We next sought to evaluate the importance of pedestal formation on murine colonization by Stx-producing *C. rodentium*. As mentioned above, infection with *C. rodentium* (Φ stx_{2dact}) resulted in high-level fecal shedding, peaking at approximately seven days post-infection, whereas fecal shedding of *C. rodentium* (Φ stx_{2dact}) tir was below detectable levels (<100 CFU/g feces) ((Mallick et al., 2012b), Table 1). Complementation of *C. rodentium* (Φ stx_{2dact}) tir with pTir_{WT} restored fecal shedding, albeit at lower levels and with delayed kinetics compared with wild type *C. rodentium* (Φ stx_{2dact}), consistent with previous results suggesting that plasmid-based complementation of *C. rodentium* (Φ stx_{2dact}) tir is incomplete ((Mallick et al., 2012b); Fig. 5A; Table 1). *C. rodentium* (Φ stx_{2dact}) tir/pTirY471F displayed further diminished fecal shedding, particularly late in infection (Fig. 5A). Pooled results of independent experiments revealed that infection with *C. rodentium* (Φ stx_{2dact}) tir/pTirY471F resulted in a five-fold decrease in peak fecal shedding compared with the isogenic *C. rodentium* (Φ stx_{2dact}) tir/pTir_{WT} (Table 1). (Peak fecal shedding of *C. rodentium* (Φ stx_{2dact}) tir/pTir_{WT} and *C. rodentium* (Φ stx_{2dact}) tir/pTirY471F was ~six- and ~four-fold higher than their non-lysogenic counterparts, respectively, consistent with the observation that lysogeny of non-toxicogenic *C. rodentium* by Φ stx_{2dact} promotes colonization; Table 1). As above, the decreased fecal shedding by *C. rodentium* (Φ stx_{2dact}) tir harboring pTirY471F was not a function of plasmid loss, because pTir_{WT} and pTirY471F were equivalently stable throughout murine infection (Sup. Table 4). Thus, a moderate decrease in fecal shedding was observed in a pedestal-defective strain, regardless of the presence or absence of Φ stx_{2dact} (see Fig. 4A-C).

To determine whether *C. rodentium* (Φ stx_{2dact}) tir/pTirY471F, displayed a more pronounced defect in colonization of the colon than of the cecum, as was the case for the non-lysogenic *C. rodentium* tir/pTirY471F, we quantified viable bacteria stably associated with each of these intestinal segments at a time point close to peak colonization. At six days post-infection, fecal shedding was ~four-fold higher in mice infected with the pedestal-competent *C. rodentium* (Φ stx_{2dact}) derivative than in mice infected with the isogenic pedestal-defective strain (Fig. 5B, **first panel**). The difference did not reach statistical significance, but was similar to the difference observed at six days post-infection in the kinetic analysis of the same strains (Fig. 5A), and to results observed for non-lysogenic *C. rodentium* derivatives (Fig. 4C, **first panel**). Likewise, a relatively small (~three-fold and statistically insignificant) difference in the concentration of the two strains in luminal washings was observed (Fig. 5B, **second panel**). Cecal colonization in mice infected with the pedestal-competent *C. rodentium* (Φ stx_{2dact}) was six-fold higher than in mice infected with the pedestal-defective strain (Fig. 5B, **third panel**), a difference nearly identical to that observed for the non-lysogenic *C. rodentium* derivatives (Fig. 4C, **third panel**), but one

that, in contrast, reached statistical significance ($p < 0.01$). Notably, colonic colonization of mice infected with the pedestal-competent strain was more than 11-fold, ($p < 0.001$) higher than in mice infected with the pedestal-defective strain (Fig. 5B, **fourth panel**). Thus, the ability to generate actin pedestals was associated with: (1) a relatively small increase in the number of bacteria present in the stool or luminal washings; (2) a modest but significant increase in colonization of the cecum; and (3) a striking and significant increase in colonization of the colon.

To assess the association of pedestal-competent and pedestal-defective *C. rodentium* ($\Phi\text{stx}_{2\text{dact}}$) with the mucosal surface during infection, we visualized infected intestinal segments by IF microscopy. At a time point near peak fecal shedding when fecal shedding of the two strains was similar, we found that the pedestal-competent *C. rodentium* ($\Phi\text{stx}_{2\text{dact}}$) adhered to the mucosal surfaces of both the cecum and the colon (Fig. 5C, **top panels**). Cecal and colonic samples of approximately 72% of mice (13/18) infected with this strain scored positive by microscopic assessment of mucosally associated *C. rodentium*, (Table 2). Bacteria closely adhered to the mucosal surface and penetrated deep into the crypts (Fig. 5C). In contrast, only 26% of cecal specimens (5/19) from mice infected with pedestal-defective *C. rodentium* scored positive, a rate ~three-fold lower than for mice infected with pedestal-competent bacteria ($p < 0.005$, Table 2; Fig. 5C). Furthermore, similar to our observation for non-toxigenic pedestal-defective *C. rodentium*, none of the 19 colonic mucosal samples scored positive, a highly significant ($p < 0.0001$) difference compared with samples from mice infected with pedestal-competent *C. rodentium* ($\Phi\text{stx}_{2\text{dact}}$). These results are also consistent with the striking (~11-fold) colonic colonization decrease seen with pedestal-defective *C. rodentium*, as assessed by viable counts (Fig. 5B). Importantly, the defect in colonization of the colonic mucosa by pedestal-defective *C. rodentium* ($\Phi\text{stx}_{2\text{dact}}$) was significantly ($p < 0.02$) greater than the defect in colonization of the cecal mucosa by this strain. Thus, pedestal-defective bacteria are significantly more impaired in colonic than in cecal colonization.

To examine more closely the interaction of pedestal-competent and pedestal-defective derivatives of *C. rodentium* ($\Phi\text{stx}_{2\text{dact}}$) with the mucosa, infected cecal and colonic tissues were evaluated by TEM. As expected, AE lesions appeared on the cecal and colonic mucosa of mice infected with *C. rodentium* ($\Phi\text{stx}_{2\text{dact}}$) *tir/pTir_{WT}* (data not shown). *C. rodentium* ($\Phi\text{stx}_{2\text{dact}}$) *tir/pTirY471F* was closely associated with the mucosal surface of the cecum, although typical AE lesions were not seen (data not shown). Consistent with our IF microscopy results, following infection with *C. rodentium* ($\Phi\text{stx}_{2\text{dact}}$) *tir/pTirY471F*, TEM revealed virtually no associated bacteria (data not shown). Thus, the ability to generate actin pedestals appears to be more critical to epithelial colonization of the colon than of the cecum.

***C. rodentium* ($\Phi\text{stx}_{2\text{dact}}$) producing TirY471F is severely diminished in the ability to cause Stx-mediated systemic disease**

The ability of pedestal-competent bacteria to colonize the colonic mucosa might be predicted to promote Stx-mediated local and systemic disease. We evaluated intestinal and renal pathology in mice infected with *C. rodentium* ($\Phi\text{stx}_{2\text{dact}}$) *tir*, *C. rodentium*

($\Phi\text{stx}_{2\text{dact}}$) *tir*/pTir_{WT}, or *C. rodentium* ($\Phi\text{stx}_{2\text{dact}}$) *tir*/pTirY471F. As previously observed, mice infected with *C. rodentium* ($\Phi\text{stx}_{2\text{dact}}$) *tir* displayed no intestinal damage (Fig. 6, **left column, arrows**; (Mallick et al., 2012b)). In contrast, infection by *C. rodentium* ($\Phi\text{stx}_{2\text{dact}}$) *tir*/pTir_{WT} resulted in destruction of the intestinal mucosa, colitis, acute ischemic injury, and inflammation at ten days post-infection (Fig. 6, **middle column, arrowheads**). Areas of necrosis and degenerative changes in the epithelial cells with crypt withering were also observed (Fig. 6, **middle column, asterisks**). As expected, the impaired ability of *C. rodentium* ($\Phi\text{stx}_{2\text{dact}}$) *tir*/pTirY471F to colonize the colonic mucosa was associated with the lack of colonic damage (Fig. 6, **right column**).

The Stx receptor Gb₃ is highly enriched in mouse renal tubules (Psotka et al., 2009). Confirming a previous report (Mallick et al., 2012b), *C. rodentium* ($\Phi\text{stx}_{2\text{dact}}$) *tir*/pTir_{WT} infection resulted in damage to the proximal tubules, reflected by flattening of the epithelial lining, the presence of pyknotic nuclear material, and sloughing of dead cells in the tubular lumen (Fig. 7A, **middle panel, arrowheads**). Mitotic activity, indicative of regeneration and repopulation of the proximal tubules, was also observed in some mice (data not shown). These pathological changes were associated with significant proteinuria (Fig. 7B). In contrast, no renal damage or proteinuria was observed upon infection with *C. rodentium* ($\Phi\text{stx}_{2\text{dact}}$) *tir*/pTirY471F (Fig. 7A, **right panel; 7B**).

Consistent with previous findings in our infection model and other murine models of Stx intoxication (Keepers et al., 2006, Sauter et al., 2008, Mohawk and O'Brien, 2011), *C. rodentium* ($\Phi\text{stx}_{2\text{dact}}$) but not *C. rodentium* ($\Phi\text{stx}_{2\text{dact}}$) *tir*, induced weight loss and death ((Mallick et al., 2012b); data not shown). pTir_{WT} complemented *C. rodentium* ($\Phi\text{stx}_{2\text{dact}}$) *tir* for these defects, but as previously observed (Mallick et al., 2012b), complementation appeared to be incomplete: Compared to mice infected with *C. rodentium* ($\Phi\text{stx}_{2\text{dact}}$), mice infected with *C. rodentium* ($\Phi\text{stx}_{2\text{dact}}$) *tir*/pTir_{WT} displayed an ~three-to-seven day delay in the kinetics of weight loss and death compared with those infected with *C. rodentium* ($\Phi\text{stx}_{2\text{dact}}$) (Fig. 7C-D; compared to Fig. 6 in reference (Mallick et al., 2012b)), and a survival rate of 37.5% vs. 0% (Table 3; (Mallick et al., 2012b); $p < 0.05$).

A rigorous logistic analysis of relative risk factors for lethal infection utilizing the relatively large number (i.e. 40) of mice infected with *C. rodentium* ($\Phi\text{stx}_{2\text{dact}}$) *tir*/pTir_{WT} revealed two critical parameters. First, the survival rate after stratification for peak fecal load revealed that a one-log increase in fecal colonization corresponded to a 5.4-fold (95% CI of 1.5- to 19.2-fold) increased risk of death (Table 3, "*C. rodentium* ($\Phi\text{stx}_{2\text{dact}}$) *tir*/pTir_{WT}"), indicating that, not surprisingly, for a given Stx-producing strain, fecal load correlates with lethality. Second, and more notably, the ability to form actin pedestals was highly associated with lethality, even after accounting for peak fecal counts. Among mice with peak fecal loads of 7.7 to 8.3 Log CFU/g feces, *C. rodentium* ($\Phi\text{stx}_{2\text{dact}}$) *tir*/pTir_{WT} infection was associated with a mortality rate of 60% (3/5), as opposed to no mortality (0/8) resulting from *C. rodentium* ($\Phi\text{stx}_{2\text{dact}}$) *tir*/pTirY471F infection (0/8; $p < 0.05$; Table 3). Similarly, for mice with peak fecal loads of 8.3 to 9.1 Log CFU/g feces, *C. rodentium* ($\Phi\text{stx}_{2\text{dact}}$) *tir*/pTir_{WT} infection resulted in a mortality rate of 53% (8/15), compared to 0% (0/5) for mice infected with *C. rodentium* ($\Phi\text{stx}_{2\text{dact}}$) *tir*/pTirY471F ($p < 0.05$; Table 3). Consistent with the stratification analysis, a logistic regression analysis showed that even when the levels of

fecal shedding were normalized, mice infected with *C. rodentium* (Φ stx_{2dact}) *tir*/pTir_{WT} were 16-fold (95% CI of 1.7-147.4-fold) more likely to succumb to lethal infection than were mice infected with the pedestal-defective *C. rodentium* (Φ stx_{2dact}) *tir*/pTirY471F strain. Thus, Tir-mediated actin pedestal formation not only promotes colonization of the colonic mucosa, but greatly facilitates Stx-mediated lethal systemic disease, even when considered independently from levels of fecal shedding.

Discussion

Tir is required for efficient cell attachment (Nougayrede et al., 2003) and for intestinal colonization by AE pathogens (Deng et al., 2003, Schauer and Falkow, 1993b, Ritchie et al., 2003, Tzipori et al., 1995, Marches et al., 2000). Tir also promotes the formation of actin pedestals, but the role of pedestals in colonization and disease has been unclear (Deng et al., 2003, Vlisidou et al., 2006, Schuller et al., 2007b). For example, an EHEC mutant lacking the type III-secreted effector EspF_U (also known as TccP; (Garmendia et al., 2004)) which, like a strain expressing TirY471F or TirY471A, was capable of Tir-mediated cell attachment but defective for pedestal formation on cultured cells, showed no discernible defect in colonization of calves or lambs (Vlisidou et al., 2006). On the other hand, an equivalent mutant displayed a mild (~2- to 6-fold, depending on the intestinal site) colonization defect in infant rabbits, and formed bacterial aggregates on the intestinal wall of infant piglets that were smaller than wild type (Ritchie et al., 2008). In a systematic analysis of the role of pedestal formation during infection, Crepin and coworkers found that *C. rodentium* producing TirY471A from a chromosomal locus formed AE lesions on colonic mucosa and was present in feces at wild type levels (Crepin et al., 2010). However, in co-infection experiments, mutant bacteria were significantly outcompeted by wild type bacteria at late time points, suggesting a colonization defect for the pedestal-incompetent mutant.

In the current study, we first investigated the role of Tir-mediated actin assembly in colonization of a mouse specifically defective for N-WASP production in the intestine. iNWKO mice were viable, fertile, displayed normal crypt-villous architecture, and exhibited no inflammatory changes. These mice were incapable of supporting mucosal colonization upon infection by *C. rodentium*, and neither *C. rodentium* nor *C. rodentium* (Φ stx_{2dact}) reached the levels of fecal bacteria found in N-WASP-proficient littermate controls. On the other hand, iNWKO mice displayed wild type sensitivity to *S. enterica* infection.

Similarly, when pedestal formation was blocked by the TirY471F bacterial mutation rather than by the iNWKO mouse mutation, fecal shedding of *C. rodentium* or *C. rodentium* (Φ stx_{2dact}) by wild type mice was reduced. (The shedding level, although reduced, was still considerably more than that observed for iNWKO mice, a finding that may indicate an additional role for N-WASP in *C. rodentium* colonization beyond pedestal formation.) The diminished fecal shedding of the pedestal-incompetent *C. rodentium tir* mutant was highly statistically significant, in contrast to the near wild type levels of fecal shedding by a strain producing TirY474A reported by Crepin and coworkers and mentioned above (Crepin et al., 2010). These investigators compared the function of a single-copy wild type or mutant *tir* alleles inserted into the endogenous chromosomal *tir* locus. In contrast, we transformed Tir-deficient strains with a Tir-encoding plasmid, which resulted in only partial

complementation. Expression of *tir* from a multicopy plasmid such as that used here may result in non-wild type levels of Tir per cell, and the efficiency of Tir translocation via the type III secretion system may be influenced by the level of Tir produced. Notably, Deng and coworkers found that infection of mice with a *C. rodentium* strain producing plasmid-encoded, pedestal-incompetent TirY471F resulted in lower than wild type bacterial titers in stool-filled colonic samples, although the 4.5-fold difference did not reach statistical significance (Deng et al., 2003). Although these investigators presented TEM evidence of AE lesions beneath bound, TirY471F-producing bacteria, a systematic IF microscopic analysis to measure the relative frequency of mucosa-associated bacteria, such as was performed in this study, was not undertaken. Regardless of the etiology of different conclusions among studies addressing the role of AE pathogen-induced pedestal formation during infection, our particular experimental system appears to be very sensitive to differences in Tir function, one that revealed a highly significant ($p < 0.001$) colonization defect of the TirY471F mutant.

Upon quantitation of bacteria associated with stool, luminal washings, cecum, or colon, production of TirY471F was associated with the most striking colonization defect in the colon (~16- and 11-fold for *C. rodentium* and *C. rodentium* (Φ stx_{2dact}), respectively) than in the cecum (~6-fold for both strains; Fig. 4, 5, Table 2). Quantitative analysis of epithelial colonization by *C. rodentium* (Φ stx_{2dact}) in the intestine, visualized by IF microscopy, revealed that the pedestal-defective mutant was associated with a significantly more severe mucosal attachment defect in the colon than in the cecum. The underlying basis for the colon-specific colonization activity of pedestal formation is not clear. The cecum is the initial colonization site for *C. rodentium* in mice (Wiles et al., 2004) and for EHEC in lambs, calves, and chickens (Wiles et al., 2004, Wales et al., 2001, Dean-Nystrom et al., 1999, Beery et al., 1985), indicating that this intestinal segment, which is a blind pouch with minimal bulk flow, may provide AE pathogens with an anatomically hospitable environment in which to establish infection (Sherman and Boedeker, 1987). We postulate that in this niche, pedestal formation is less critical for successful mucosal colonization.

The ability of a pedestal-defective AE pathogen to colonize the cecum might be predicted to mute any decrease in fecal shedding due to a defect in colonization of other intestinal segments. In fact, we found that the 11- to 16-fold defect in colonic colonization was associated with only a ~4-fold defect in fecal shedding, possibly due to luminal bacteria released from the (efficiently colonized) cecum. Given that many studies utilize fecal shedding as a convenient serial readout of intestinal colonization (Crepin et al., 2010, Vlisidou et al., 2006, Girard et al., 2009, Mundy et al., 2004, Marches et al., 2005, Ritchie and Waldor, 2005), our finding that pedestal formation may play an essential role in mucosal colonization for only a subset of intestinal segments could partially explain varying apparent defects in colonization by pedestal-defective mutants in other studies.

Pedestal formation might promote colonic colonization by any of several mechanisms. First, by promoting (indirect) attachment of the bacterium to the host cytoskeleton, pedestal formation may stabilize bacterial binding at the cell surface. Indeed, whereas we found that *C. rodentium* (Φ stx_{2dact}) expressing TirY471F bound to cultured murine cells indistinguishably from *C. rodentium* (Φ stx_{2dact}) producing wild type Tir, the ability of

EHEC to promote actin assembly is associated with enhanced binding to cultured mammalian cells (S. Battle and G. Hecht, personal communication). This putative stable attachment, in addition to facilitating intestinal retention of *C. rodentium* in the face of luminal bulk flow, may allow the pathogen to occupy an environmental niche protected from intense nutritional competition with commensal bacteria located in the lumen (Kamada et al., 2012). Second, N-WASP has been previously shown to promote type III secretion by EHEC and (to a lesser degree) EPEC (Vingadassalom et al., 2010). In addition, a mutation in EHEC Tir that diminishes actin pedestal formation is associated with a moderate (but significant) defect in type III translocation (S. Battle and G. Hecht, personal communication). These findings raise the possibility that, given the requirement of effector translocation for efficient colonization (Ritchie and Waldor, 2005, Deng et al., 2004), the defect in *C. rodentium* colonization observed in the iNWKO mice may in part be due to diminished type III translocation. Finally, the dynamic nature of actin turnover and assembly in pedestals promotes the movement of EHEC or EPEC on the surface of cultured mammalian cells (Sanger et al., 1996, Shaner et al., 2005), and similar to actin-based cell-to-cell spread of *Vaccinia* virus (Goldberg, 2001), pedestal formation may promote the spread of the pathogen, consistent with the smaller than wild type aggregates of pedestal-defective EHEC on the mucosal surface (Ritchie et al., 2008).

The enhanced mucosal colonization facilitated by actin pedestal formation was associated with dramatically greater Stx-mediated pathogenicity. First, iNWKO mice exhibited less intestinal and renal damage, maintained body weight, and uniformly survived infection by *C. rodentium* (Φ stx_{2dact}), in contrast to N-WASP-proficient littermate controls, who lost weight and suffered a 35% lethality rate. Second, mice infected with pedestal-defective *C. rodentium* (Φ stx_{2dact}) demonstrated less intestinal damage and no renal dysfunction or weight loss. The dramatically enhanced Stx-mediated disease induced by pedestal-competent *C. rodentium* (Φ stx_{2dact}) was not simply a function of bacterial load in the lumen, because pedestal-competent *C. rodentium* (Φ stx_{2dact}) was associated with a 16-fold greater risk of death compared to pedestal-defective bacteria after normalizing for the peak fecal load of bacteria.

Although we cannot rule out the possibility that bacteria bound to the mucosal surface produce more Stx than luminal bacteria, it is also possible that pedestal formation directly or indirectly facilitates Stx penetration of the epithelial barrier, leading to systemic intoxication (Nakao and Takeda, 2000). For example, type III effectors such as EspF disrupt the epithelial barrier (Guttman et al., 2006, Holmes et al., 2010, McNamara et al., 2001), and as mentioned above, pedestal formation promotes not only EHEC attachment but also the efficiency of effector translocation per bound EHEC (S. Battle and G. Hecht., pers. comm.). In addition, pedestal formation, by disrupting the apical actin network, may itself compromise tight junctions, as several tight junction components are aberrantly localized to pedestals on cultured cells (Peralta-Ramirez et al., 2008, Hanajima-Ozawa et al., 2007). Finally, the proximity of Stx production at the mucosal surface, perhaps in combination with the intestinal damage observed in this infection (Mallick et al., 2012b), may promote toxemia. Interestingly, infection by the recently emerged *E. coli* O104:H4, a Stx-producing strain that is related to enteroaggregative *E. coli* (EAEC), is associated with a high rate of

rapidly progressing Stx-mediated disease and HUS (Rasko et al., 2011). This strain is incapable of generating AE lesions, indicating that AE lesion formation is not an absolute requirement for Stx-mediated disease. Nevertheless, like EAEC, *E. coli* O104:H4 is highly adherent to cultured host cells (Pierard et al., 2012, Beutin and Martin, 2012), suggesting that Stx production in the context of tight bacterial adherence may promote severe Stx-mediated disease (Bielaszewska et al., 2011). Thus, future investigation into the relationship between mucosal colonization promoted by actin pedestal formation and systemic disease promoted by Stx may provide general insights into the pathogenesis of toxigenic mucosal pathogens.

Materials and Methods

Phage and bacterial strains

Bacterial and phage strains used in this study are listed in Sup. Table 1. The phage used to generate *C. rodentium* (Φ *stx*_{2dact}) was Φ 1720a-02 *Rz::cat* (Sup. Table 1), derived from STEC strain EC1720 (Gobius et al., 2003). EC1720 was originally thought to be lysogenized by a single Stx-producing phage, Φ 1720a (Gobius et al., 2003), also termed Φ 1720a-01 (Mallick et al., 2012b). We subsequently showed that EC1720 was also lysogenized by a second Stx-producing phage, Φ 1720a-02, this one producing *stx*_{2dact} (Mallick et al., 2012b). A chloramphenicol resistance cassette was then inserted into the *Rz* locus of Φ 1720a-02 to generate the *stx*_{2dact}-producing phage Φ 1720a-02 *Rz::cat* (Mallick et al., 2012b). This latter phage was originally termed “ λ *stx*_{2dact}” (Mallick et al., 2012b). However, subsequent DNA sequencing and annotation of Φ 1720a-02 *Rz::cat* *stx*_{2dact}:*kan*, a derivative of Φ 1720a-02 *Rz::cat* harboring a kanamycin resistance cassette in *stx*_{2dact}, revealed that Φ 1720a-02 (GenBank accession number KF03044) is only distantly related to phage λ (M. Osburne and A. Tai, personal communication). Therefore, we have removed “ λ ” from all designations of this phage and now denote it as “ Φ *stx*_{2dact}”.

Bacterial growth conditions

Bacterial strains were cultured in Luria-Bertani broth (LB) (Miller) at 37°C, unless indicated otherwise. Antibiotics were used at the following concentrations: kanamycin, 25 μ g/ml; zeocin, 75 μ g/ml; chloramphenicol, 10 μ g/ml; tetracycline, 5 μ g/ml; and streptomycin, 20 μ g/ml.

Plasmid isolation, primers, and sequencing

Plasmids used this study are listed in Sup. Table 2. Plasmid DNA was isolated using the QIAprep Spin Miniprep Kit (QIAGEN, Valencia, CA). Primers were purchased from Invitrogen (Grand Island, NY) and are listed in Sup. Table 3. Sequencing was performed at Tufts University Core Sequencing Facility (Boston, MA).

Construction of a *C. rodentium* TirY471F plasmid

pEM340 “pTirY471F” was constructed using SLIM as previously described (Chiu et al., 2004), using the following primers: R-Oli178, F-Oli179, R-Oli180, and F-Oli181 (Sup. Table 3). Plasmid constructs were confirmed by sequencing and pedestal formation was

tested by phalloidin and DAPI staining of infected monolayers as previously described (Mallick et al., 2012a).

Infection and binding analysis of *C. rodentium* (Φ stx_{2dact}) and mutants on cultured cells

Filamentous actin staining (FAS) assay and bacterial binding quantification was done as previously described (Mallick et al., 2012a).

Generation, characterization, and infection of conditional, intestinal, N-WASP^{-/-} mice

The PCR strategy for developing and genotyping the iNWKO mouse has been previously described (Lyubimova et al., 2010, Cotta-de-Almeida et al., 2007). iNWKO breeder mice and offspring were housed at the UMass Medical School (UMMS) animal facility, the Center for Comparative Medicine at the Massachusetts General Hospital, and/or the Boston Children's Hospital animal facility. iNWKO mice were generated by breeding female conditionally targeted *N-Wasp*^{flox/flox} mice, in which exon 2 of N-WASP is flanked by LoxP sites (Cotta-de-Almeida et al., 2007, Lyubimova et al., 2010), with transgenic male *N-Wasp*^{flox/+}, *tg*^{villin-Cre} mice expressing Cre recombinase under the intestine-specific promoter villin (el Marjou et al., 2004). This breeding resulted in approximately 15% of mice with the desired genotype (*N-wasp*^{flox/flox}, *tg*^{villin-Cre}). Genotyping was performed by Transnetyx (Cordova, TN). Throughout the text, littermate control mice are defined as those mice in the same litter as the iNWKO mice with any of the following genotypes: *N-Wasp*^{+/+}, *N-Wasp*^{flox/+}, *N-Wasp*^{flox/flox}, or *N Wasp*^{flox/+}, *tg*^{villin-Cre}.

For Western blotting, intestinal epithelial cells (IECs) were isolated from eight-week old littermate control or iNWKO mice by EDTA dissociation, as previously described (Whitehead and Robinson, 2009), and lysed with ice-cold RIPA buffer (Tris 50 mM, NaCl 150 mM, SDS 0.1%, sodium deoxycholate 0.5%, NP-40 1%, complete protease inhibitor cocktail). IEC protein extracts were separated by SDS gel electrophoresis, and transferred onto nitrocellulose membrane as previously described (Campellone et al., 2008). Immunoblotting was performed with rabbit polyclonal anti-N-WASP (1:2000) (kindly provided by Dr. Marc Kirshner), followed by HRP-conjugated goat anti-rabbit secondary antibody (1:3000) (Cell Signaling, Danvers, MA), and visualized using enhanced chemiluminescence (ECL) (GE Healthcare Life Sciences, Piscataway, NJ).

All infection experiments using iNWKO mice were approved by UMMS Department of Animal Medicine and the UMMS IACUC (protocol-2049 to JML and A-1993-11 to BAM), the Subcommittee on Research Animal Care of the Massachusetts General Hospital (protocol-2005N000266), and the Children's Hospital Animal Care and Use Committee (protocol-11-04-1918). The murine infection experiments included age and sex matched littermate controls. Inoculum doses for infection of iNWKO mice and littermate controls were $\sim 5 \times 10^8$ CFU and $\sim 1 \times 10^9$ CFU for GFP-*C. rodentium* and *C. rodentium* (Φ stx_{2dact}), respectively. Fecal shedding, percent body weight loss, and proteinuria indices were determined as previously described (Mallick et al., 2012b). Maximal fecal shedding was defined as the highest titer of bacteria in the stool at any time point throughout the course of infection. Maximal percent body weight loss was defined as the maximum amount lost at any time point throughout the course of experiment. Note that mice that had suffered weight

loss and proteinuria but survived infection ultimately cleared intestinal bacteria, regained weight to original baseline, and recovered from proteinuria. However, the rate of clinical recovery of individual mice was somewhat slower than that which might be inferred from graphs of average post-infection weight loss and proteinuria (Figures 3E, 7B and C), because mice with the most severe weight loss and proteinuria were euthanized, thus enriching the set of surviving mice for those that were less affected by infection. Hence, the depicted average post-infection weight and proteinuria, which reflects this set of surviving mice, returned toward baseline more quickly than the weight and proteinuria of individual mice.

For IF, sections from the proximal and distal colon were embedded in OCT and 5 μ m frozen sections were electrostatically adhered to glass slides. Upon reaching room temperature, slides were fixed in 4% paraformaldehyde for 10 minutes, stained with phalloidin, and mounted with Vectashield mounting medium with DAPI (Vector Laboratories, Burlingame, CA). Histological and IF identification of GFP+ bacteria was performed using an Olympus AX-70 upright fluorescence microscope (Olympus, Tokyo, Japan).

To quantify the intercrypt mucosal epithelium with adherent *C. rodentium*, intestinal sections from wild type and iNWKO mice were taken at four days post-infection with GFP-expressing *C. rodentium* (see Sup. Table 1). Sections were flash frozen in OCT and sectioned at 5 μ m. Slides were fixed in 4% paraformaldehyde, stained with DAPI, and visualized with an upright epifluorescence microscope. Four sections from each tissue sample were examined, and the mucosal epithelium located between adjacent crypts (designated the intercrypt mucosal epithelium, ICME) was examined for the presence of adherent, GFP-positive bacteria. The mean percentage of ICME demonstrating intimately adherent bacteria per section was calculated. At least 30 ICME per section were examined.

To determine whether decreased colonization of iNWKO mice with wild type *C. rodentium* was due specifically to the absence of N-WASP rather than as a consequence of globally altered intestinal physiology (e.g., altered underlying immune reactivity or defective antimicrobial peptide secretion), littermate control and iNWKO mice were infected with 1.6×10^8 CFU *Salmonella* by oral gavage, as previously described (Srikanth et al., 2010). Bacterial recovery from tissue or stool in iNWKO compared to littermate control mice was quantitated by viable counts. Tissues were processed for histology and evaluated as previously described (Mallick et al., 2012b).

Infection of wild type mice with engineered *C. rodentium* strains expressing wild type or mutant Tir

Wild type mice were purchased from Jackson Laboratories (Bar Harbor, ME) and housed in the UMMS animal facility. Eight-week old, female, C57BL/6J mice were infected as previously described (Mallick et al., 2012b). All experimental groups contained at least five mice unless otherwise stated. The animal protocol (A-2049) was approved by the UMMS Department of Animal Medicine and the UMMS IACUC. Fecal shedding, weight loss, and proteinuria indices were determined as previously described (Mallick et al., 2012b).

Determination of peak fecal shedding of bacteria

The kinetics of fecal shedding occasionally differed from experiment to experiment even accounting for bacterial and murine strain, so for some comparisons we scored the peak of fecal shedding during the course of infection instead of shedding on a particular day after inoculation. In some instances, results from multiple experiments were pooled in order to increase the discrimination of statistically significant differences.

Determination of plasmid retention during murine infection

To assess the loss of Tir-producing plasmids during murine infection, groups of three mice were infected with *C. rodentium* tir/pTir_{WT}, *C. rodentium* tir/pTirY471F, *C. rodentium* (Φ stx_{2dact}) tir/pTir_{WT}, or *C. rodentium* (Φ stx_{2dact}) tir/pTirY471F. Feces were collected on days five, seven, ten and twelve days post-infection. Fecal counts were determined by serial dilution and plating on MacLac (*C. rodentium*) or LB chloramphenicol (*C. rodentium* (Φ stx_{2dact}) strains) plates, and the percent plasmid retention for each strain was determined by patching 100 colonies on to LB kanamycin plates. Plasmid retention was calculated by dividing the number of patched colonies that grew on kanamycin by the total number of colonies that grew on the MacLac or LB chloramphenicol plates, then multiplying by 100.

Analysis of tissue damage and bacterial association with mucosal surfaces by *C. rodentium* producing wild type or mutant Tir

Tissues were processed for histology and evaluated as previously described (Mallick et al., 2012b). For IF staining, at the indicated time post-infection, cecal or colonic sections were stained with DAPI to identify cell nuclei and anti-*Citrobacter* antibody (1:1600; a gift from David Schauer (Borenshtein et al., 2008)). Samples were taken at six days post-infection for quantification of the IF samples (Table 2) and fecal counts at this time point were between 1.3×10^5 and 4.0×10^8 CFU per gram of stool for mice infected with the non-toxicogenic *C. rodentium* strains and between 1.3×10^5 and 1.3×10^9 CFU per gram of stool for mice infected with the toxigenic *C. rodentium* (Φ stx_{2dact}) strains. To generate a score for epithelial colonization for each intestinal segment (Table 2), approximately ten fields of cecal or colonic samples from each infected mouse were visualized microscopically for approximately five minutes and scored for bacteria adherent to the epithelium. The observation of one or more *C. rodentium* associated with the mucosal surface of a given segment resulted in a positive score for epithelial colonization of that segment. Data in Table 2 were compiled from three independent experiments using three-to-ten mice per group for each of the strains. Statistical significance was determined by a Student's t-test. TEM was performed as previously described (Mallick et al., 2012a, Mallick et al., 2012b).

Determination of CFU associated with different intestinal segments

At necropsy, the large intestine and fecal contents were removed. The large intestine was flushed with 1 ml PBS to remove loosely bound bacteria. Contents of the flush ("luminal washings") were collected and serial dilutions were plated on LB agar (\pm antibiotic). The intestine was divided into two parts: cecum and colon, homogenized, and serial dilutions were plated on LB agar (\pm antibiotic) to quantify the number of bacteria/mg of tissue.

Purification and generation of an anti-*Citrobacter* Tir antibody

Generation of an anti-*Citrobacter* Tir antibody was similar to the generation of an anti-EHEC Tir antibody, as previously described (Mallick et al., 2012a) with the exception that a *C. rodentium* Tir expression vector (pEM385 “pCrTirExp”) was used. Primers F-190 and R-191 were used to amplify *C. rodentium tir* with *Nde*I and *Sal*I flanking restriction sites (1.644 kb) from pEM129 “pTir_{WT}”. This PCR fragment was cloned into the *Nde*I and *Sal*I sites of plasmid pET21b and transformed into *E. coli* DH5 α . Transformants were selected on plates containing ampicillin. Candidate clones were verified by restriction digestion, PCR with primers R-iTirL and F-iTirU (480 bp), and sequencing. Upon sequence verification, pCrTirExp was transformed into BL21 DE3 and purified as previously described (Mallick et al., 2012a).

Tir immunoblotting

C. rodentium strains were cultured in DMEM + 0.1M HEPES at 37°C, 5% CO₂ for 4.5 hours. After centrifuging at 22,000 \times g for 10 minutes at room temperature, media was decanted and trichloroacetic acid was added in a 1:1 volume and incubated overnight at -20°C. The sample was then centrifuged at 22,000 \times g for 10 minutes at 4°C, the supernatant was decanted, and the pellet was resuspended in acetone and centrifuged at 20,800 \times g at 4°C for 10 minutes. Acetone was decanted and the pellet was air dried for 10 minutes and resuspended in water. Gel loading for SDS-PAGE was standardized to either final protein concentration quantified by Nanodrop (Thermo Fisher Scientific Inc., Wilmington, DE) or final OD₆₀₀.

Stratification of colonization intervals

To compare the degree of lethality between mice infected with *C. rodentium* (Φ stx_{2dact}) *tir*/pTir and *C. rodentium* (Φ stx_{2dact}) *tir*/pTirY471F at equivalent levels of fecal shedding, animals were grouped into five strata depending on peak fecal shedding levels (i.e. 9.7-10.7 Log CFU/g, 9.1-9.7 Log CFU/g, 8.3-9.1 Log CFU/g, 7.7-8.3 Log CFU/g, and below 7.7 CFU/g) (see Table 3). This grouping allowed for the maximum number of mice infected with each strain per grouping and the mean peak fecal colonization level within each grouping was nearly identical both in mice infected with *C. rodentium* (Φ stx_{2dact}) *tir*/pTir and with *C. rodentium* (Φ stx_{2dact}) *tir*/pTirY471F. However, grouping of mice into two or three (rather than five) strata on the basis of peak fecal colonization also supported the conclusion that pedestal formation promotes lethality (S. Baker and E.M., data not shown).

Statistical analysis

Differences in outcomes between strains were evaluated using Student's t-tests for two group comparisons, and one-way and two-factor repeated measures ANOVA appropriately for more complex designs. In the presence of significant effects, pairwise comparisons were made using Tukey's HSD multiple comparisons procedure in the case of the one-way ANOVA, and Bonferroni adjusted Fisher's LSD tests in the case of the two-factor repeated measures ANOVA. Dichotomous categorical outcomes were modeled using logistic regression analysis using likelihood ratio chi-square tests to evaluate the significance of model terms. Differences in survival times were evaluated using Kaplan Meier Product

Moment Survival Analysis with Log Rank tests to evaluate significance. Multivariate survival analysis was performed using Cox Proportionate Hazards models. The proportionate hazards assumption was tested by visual inspection of cumulative survival plots. Statistical significance was defined as effects with p-values less than or equal to 0.05. *= $p < 0.05$, **= $p < 0.01$, ***= $p < 0.001$. Analyses were performed using GraphPad Prism and SPSS version 15.

Supplementary Material

Refer to Web version on PubMed Central for supplementary material.

Acknowledgments

We thank Z. Demma for invaluable assistance with *Salmonella* infection of mice. We thank the UMMS DERC for processing tissue for histology, L. Strittmatter and G. Hendricks of the UMMS EM Core for processing EM samples, L. Sonenshein and M. Osburne for thoughtful comments on the manuscript, Stephen Baker of UMMS for help with statistical analyses, Marc Kirshner for the N-WASP antibody, and the Tufts University CTSI consultative services. Electron microscopy on littermate control and iNWKO mice was performed in the Microscopy Core of the Center for Systems Biology/Program in Membrane Biology, which is partially supported by an Inflammatory Bowel Disease Grant DK43351 and a Boston Area Diabetes and Endocrinology Research Center (BADERC) Award DK57521. The work in this manuscript was supported by NIH grants R21 AI092009 and R01 AI46454 to JML, NIH grants P01 HL059561, R01 AI052354, 5P30DK034854 to SBS, NIH grant K08 DK094966 to JJG, a Career Development Award from the Crohn's and Colitis Foundation of America to JJG, NIH grants to DK56754 and DK33506 BAM, and by the National Center for Research Resources Grant Number UL1 RR025752 and the National Center for Advancing Translational Sciences, National Institutes of Health, Grant Number UL1 TR000073 to Tufts University CTSI consultative services.

Dedication: This work is dedicated to the memory of David Schauer, who was critical to its initiation.

References

- BEERY JT, DOYLE MP, SCHOENI JL. Colonization of chicken cecae by *Escherichia coli* associated with hemorrhagic colitis. *Applied and environmental microbiology*. 1985; 49:310–5. [PubMed: 3885853]
- BEUTIN L, MARTIN A. Outbreak of Shiga toxin-producing *Escherichia coli* (STEC) O104:H4 infection in Germany causes a paradigm shift with regard to human pathogenicity of STEC strains. *Journal of food protection*. 2012; 75:408–18. [PubMed: 22289607]
- BIELASZEWSKA M, MELLMANN A, ZHANG W, KOCK R, FRUTH A, BAUWENS A, PETERS G, KARCH H. Characterisation of the *Escherichia coli* strain associated with an outbreak of haemolytic uraemic syndrome in Germany, 2011: a microbiological study. *The Lancet infectious diseases*. 2011; 11:671–6. [PubMed: 21703928]
- BORENSHTEIN D, MCBEE ME, SCHAUER DB. Utility of the *Citrobacter rodentium* infection model in laboratory mice. *Curr Opin Gastroenterol*. 2008; 24:32–7. [PubMed: 18043230]
- BRADY MJ, CAMPELLONE KG, GHILDIYAL M, LEONG JM. Enterohaemorrhagic and enteropathogenic *Escherichia coli* Tir proteins trigger a common Nck-independent actin assembly pathway. *Cell Microbiol*. 2007; 9:2242–53. [PubMed: 17521329]
- CAMPELLONE KG. Cytoskeleton-modulating effectors of enteropathogenic and enterohaemorrhagic *Escherichia coli*: Tir, EspFu and actin pedestal assembly. *FEBS J*. 2010; 277:2390–402. [PubMed: 20477869]
- CAMPELLONE KG, CHENG HC, ROBBINS D, SIRIPALA AD, MCGHIE EJ, HAYWARD RD, WELCH MD, ROSEN MK, KORONAKIS V, LEONG JM. Repetitive N-WASP-binding elements of the enterohemorrhagic *Escherichia coli* effector EspF(U) synergistically activate actin assembly. *PLoS pathogens*. 2008; 4:e1000191. [PubMed: 18974829]
- CAMPELLONE KG, GIESE A, TIPPER DJ, LEONG JM. A tyrosine phosphorylated 12-amino-acid sequence of enteropathogenic *Escherichia coli* Tir binds the host adaptor protein Nck and is

- required for Nck localization to actin pedestals. *Mol Microbiol.* 2002; 43:1227–41. [PubMed: 11918809]
- CAMPELLONE KG, LEONG JM. Nck-independent actin assembly is mediated by two phosphorylated tyrosines within enteropathogenic *Escherichia coli* Tir. *Mol Microbiol.* 2005; 56:416–32. [PubMed: 15813734]
- CAMPELLONE KG, RANKIN S, PAWSON T, KIRSCHNER MW, TIPPER DJ, LEONG JM. Clustering of Nck by a 12-residue Tir phosphopeptide is sufficient to trigger localized actin assembly. *J Cell Biol.* 2004a; 164:407–16. [PubMed: 14757753]
- CAMPELLONE KG, ROBBINS D, LEONG JM. EspF_U is a translocated EHEC effector that interacts with Tir and N-WASP and promotes Nck-independent actin assembly. *Dev Cell.* 2004b; 7:217–28. [PubMed: 15296718]
- CARON E, CREPIN VF, SIMPSON N, KNUTTON S, GARMENDIA J, FRANKEL G. Subversion of actin dynamics by EPEC and EHEC. *Curr Opin Microbiol.* 2006; 9:40–5. [PubMed: 16406772]
- CHIU J, MARCH PE, LEE R, TILLET D. Site-directed, Ligase-Independent Mutagenesis (SLIM): a single-tube methodology approaching 100% efficiency in 4 h. *Nucleic acids research.* 2004; 32:e174. [PubMed: 15585660]
- COTTA-DE-ALMEIDA V, WESTERBERG L, MAILLARD MH, ONALDI D, WACHTEL H, MEELU P, CHUNG UI, XAVIER R, ALT FW, SNAPPER SB. Wiskott Aldrich syndrome protein (WASP) and N-WASP are critical for T cell development. *Proceedings of the National Academy of Sciences of the United States of America.* 2007; 104:15424–9. [PubMed: 17878299]
- CREPIN VF, GIRARD F, SCHULLER S, PHILLIPS AD, MOUSNIER A, FRANKEL G. Dissecting the role of the Tir:Nck and Tir:IRTKS/IRSp53 signalling pathways *in vivo*. *Mol Microbiol.* 2010; 75:308–23. [PubMed: 19889090]
- CROXEN MA, FINLAY BB. Molecular mechanisms of *Escherichia coli* pathogenicity. *Nature reviews. Microbiology.* 2010; 8:26–38.
- DE GRADO M, ABE A, GAUTHIER A, STEELE-MORTIMER O, DEVINNEY R, FINLAY BB. Identification of the intimin-binding domain of Tir of enteropathogenic *Escherichia coli*. *Cell Microbiol.* 1999; 1:7–17. [PubMed: 11207537]
- DEAN-NYSTROM EA, BOSWORTH BT, MOON HW. Pathogenesis of *Escherichia coli* O157:H7 in weaned calves. *Advances in experimental medicine and biology.* 1999; 473:173–7. [PubMed: 10659355]
- DENG W, PUENTE JL, GRUENHEID S, LI Y, VALLANCE BA, VAZQUEZ A, BARBA J, IBARRA JA, O'DONNELL P, METALNIKOV P, ASHMAN K, LEE S, GOODE D, PAWSON T, FINLAY BB. Dissecting virulence: systematic and functional analyses of a pathogenicity island. *Proc Natl Acad Sci U S A.* 2004; 101:3597–602. [PubMed: 14988506]
- DENG W, VALLANCE BA, LI Y, PUENTE JL, FINLAY BB. *Citrobacter rodentium* translocated intimin receptor (Tir) is an essential virulence factor needed for actin condensation, intestinal colonization and colonic hyperplasia in mice. *Mol Microbiol.* 2003; 48:95–115. [PubMed: 12657048]
- DONNENBERG MS, TACKET CO, JAMES SP, LOSONSKY G, NATARO JP, WASSERMAN SS, KAPER JB, LEVINE MM. Role of the *eaeA* gene in experimental enteropathogenic *Escherichia coli* infection. *J Clin Invest.* 1993; 92:1412–7. [PubMed: 8376594]
- EL MARJOU F, JANSSEN KP, CHANG BH, LI M, HINDIE V, CHAN L, LOUVARD D, CHAMBON P, METZGER D, ROBINE S. Tissue-specific and inducible Cre-mediated recombination in the gut epithelium. *Genesis.* 2004; 39:186–93. [PubMed: 15282745]
- FRANKEL G, PHILLIPS AD. Attaching effacing *Escherichia coli* and paradigms of Tir-triggered actin polymerization: getting off the pedestal. *Cellular microbiology.* 2008; 10:549–56. [PubMed: 18053003]
- GARMENDIA J, FRANKEL G, CREPIN VF. Enteropathogenic and enterohemorrhagic *Escherichia coli* infections: translocation, translocation, translocation. *Infect Immun.* 2005; 73:2573–85. [PubMed: 15845459]
- GARMENDIA J, PHILLIPS AD, CARLIER MF, CHONG Y, SCHULLER S, MARCHES O, DAHAN S, OSWALD E, SHAW RK, KNUTTON S, FRANKEL G. TccP is an

- enterohaemorrhagic *Escherichia coli* O157:H7 type III effector protein that couples Tir to the actin-cytoskeleton. *Cell Microbiol.* 2004; 6:1167–83. [PubMed: 15527496]
- GHAEM-MAGHAMI M, SIMMONS CP, DANIELL S, PIZZA M, LEWIS D, FRANKEL G, DOUGAN G. Intimin-specific immune responses prevent bacterial colonization by the attaching-effacing pathogen *Citrobacter rodentium*. *Infection and immunity.* 2001; 69:5597–605. [PubMed: 11500434]
- GIRARD F, CREPIN VF, FRANKEL G. Modelling of infection by enteropathogenic *Escherichia coli* strains in lineages 2 and 4 ex vivo and *in vivo* by using *Citrobacter rodentium* expressing TccP. *Infect Immun.* 2009; 77:1304–14. [PubMed: 19188355]
- GOBIUS KS, HIGGS GM, DESMARCHELIER PM. Presence of activatable Shiga toxin genotype (stx2d) in Shiga toxigenic *Escherichia coli* from livestock sources. *J Clin Microbiol.* 2003; 41:3777–83. [PubMed: 12904389]
- GOLDBERG MB. Actin-based motility of intracellular microbial pathogens. *Microbiol Mol Biol Rev.* 2001; 65:595–626. table of contents. [PubMed: 11729265]
- GRUENHEID S, DEVINNEY R, BLADT F, GOOSNEY D, GELKOP S, GISH GD, PAWSON T, FINLAY BB. Enteropathogenic *E. coli* Tir binds Nck to initiate actin pedestal formation in host cells. *Nat Cell Biol.* 2001; 3:856–9. [PubMed: 11533668]
- GUTTMAN JA, SAMJI FN, LI Y, VOGL AW, FINLAY BB. Evidence that tight junctions are disrupted due to intimate bacterial contact and not inflammation during attaching and effacing pathogen infection *in vivo*. *Infect Immun.* 2006; 74:6075–84. [PubMed: 16954399]
- HANAJIMA-OZAWA M, MATSUZAWA T, FUKUI A, KAMITANI S, OHNISHI H, ABE A, HORIGUCHI Y, MIYAKE M. Enteropathogenic *Escherichia coli*, *Shigella flexneri*, and *Listeria monocytogenes* recruit a junctional protein, zonula occludens-1, to actin tails and pedestals. *Infection and immunity.* 2007; 75:565–73. [PubMed: 17118974]
- HARTLAND EL, BATCHELOR M, DELAHAY RM, HALE C, MATTHEWS S, DOUGAN G, KNUTTON S, CONNERTON I, FRANKEL G. Binding of intimin from enteropathogenic *Escherichia coli* to Tir and to host cells. *Molecular microbiology.* 1999; 32:151–8. [PubMed: 10216868]
- HAYWARD RD, LEONG JM, KORONAKIS V, CAMPELLONE KG. Exploiting pathogenic *Escherichia coli* to model transmembrane receptor signalling. *Nat Rev Microbiol.* 2006; 4:358–70. [PubMed: 16582930]
- HOLMES A, MUHLEN S, ROE AJ, DEAN P. The EspF effector, a bacterial pathogen's Swiss army knife. *Infection and immunity.* 2010; 78:4445–53. [PubMed: 20679436]
- KAMADA N, KIM YG, SHAM HP, VALLANCE BA, PUENTE JL, MARTENS EC, NUNEZ G. Regulated virulence controls the ability of a pathogen to compete with the gut microbiota. *Science.* 2012; 336:1325–9. [PubMed: 22582016]
- KAPER JB, NATARO JP, MOBLEY HL. Pathogenic *Escherichia coli*. *Nat Rev Microbiol.* 2004; 2:123–40. [PubMed: 15040260]
- KARMALI MA, GANNON V, SARGEANT JM. Verocytotoxin-producing *Escherichia coli* (VTEC). *Vet Microbiol.* 2009; 140:360–70. [PubMed: 19410388]
- KEEPERS TR, PSOTKA MA, GROSS LK, OBRIG TG. A murine model of HUS: Shiga toxin with lipopolysaccharide mimics the renal damage and physiologic response of human disease. *J Am Soc Nephrol.* 2006; 17:3404–14. [PubMed: 17082244]
- KENNY B. Phosphorylation of tyrosine 474 of the enteropathogenic *Escherichia coli* (EPEC) Tir receptor molecule is essential for actin nucleating activity and is preceded by additional host modifications. *Mol Microbiol.* 1999; 31:1229–41. [PubMed: 10096089]
- KENNY B, DEVINNEY R, STEIN M, REINSCHIED DJ, FREY EA, FINLAY BB. Enteropathogenic *E. coli* (EPEC) transfers its receptor for intimate adherence into mammalian cells. *Cell.* 1997; 91:511–20. [PubMed: 9390560]
- LOMMEL S, BENESCH S, ROTTNER K, FRANZ T, WEHLAND J, KUHN R. Actin pedestal formation by enteropathogenic *Escherichia coli* and intracellular motility of *Shigella flexneri* are abolished in N-WASP-defective cells. *EMBO Rep.* 2001; 2:850–7. [PubMed: 11559594]
- LYUBIMOVA A, GARBER JJ, UPADHYAY G, SHAROV A, ANASTASOAI F, YAJNIK V, COTSARELIS G, DOTTO GP, BOTCHKAREV V, SNAPPER SB. Neural Wiskott-Aldrich

syndrome protein modulates Wnt signaling and is required for hair follicle cycling in mice. *The Journal of clinical investigation*. 2010; 120:446–56. [PubMed: 20071778]

- MALLICK EM, BRADY MJ, LUPERCHIO SA, VANGURI V, MAGOUN L, LIU H, SHEPPARD BJ, MUKHERJEE J, DONOHUE-ROLFE A, TZIPORI S, LEONG JM, SCHAUER DB. Allele- and Tir-independent functions of intimin in diverse animal infection models. *Frontiers in microbiology*. 2012a; 3
- MALLICK EM, MCBEE ME, VANGURI VK, MELTON-CELSA AR, SCHLIEPER K, KARALIUS BJ, O'BRIEN AD, BUTTERTON JR, LEONG JM, SCHAUER DB. A novel murine infection model for Shiga toxin-producing *Escherichia coli*. *The Journal of clinical investigation*. 2012b
- MARCHES O, NOUGAYREDE JP, BOULLIER S, MAINIL J, CHARLIER G, RAYMOND I, POHL P, BOURY M, DE RYCKE J, MILON A, OSWALD E. Role of Tir and intimin in the virulence of rabbit enteropathogenic *Escherichia coli* serotype O103:H2. *Infect Immun*. 2000; 68:2171–82. [PubMed: 10722617]
- MARCHES O, WILES S, DZIVA F, LA RAGIONE RM, SCHULLER S, BEST A, PHILLIPS AD, HARTLAND EL, WOODWARD MJ, STEVENS MP, FRANKEL G. Characterization of two non-locus of enterocyte effacement- encoded type III-translocated effectors, NleC and NleD, in attaching and effacing pathogens. *Infection and immunity*. 2005; 73:8411–7. [PubMed: 16299341]
- MCDANIEL TK, JARVIS KG, DONNENBERG MS, KAPER JB. A genetic locus of enterocyte effacement conserved among diverse enterobacterial pathogens. *Proc Natl Acad Sci U S A*. 1995; 92:1664–8. [PubMed: 7878036]
- MCNAMARA BP, KOUTSOURIS A, O'CONNELL CB, NOUGAYREDE JP, DONNENBERG MS, HECHT G. Translocated EspF protein from enteropathogenic *Escherichia coli* disrupts host intestinal barrier function. *J Clin Invest*. 2001; 107:621–9. [PubMed: 11238563]
- MELTON-CELSA A, MOHAWK K, TEEL L, O'BRIEN A. Pathogenesis of Shiga-Toxin Producing *Escherichia coli*. *Current topics in microbiology and immunology*. 2011
- MOHAWK KL, O'BRIEN AD. Mouse models of *Escherichia coli* O157:H7 infection and shiga toxin injection. *Journal of biomedicine & biotechnology*. 2011; 2011:258185. [PubMed: 21274267]
- MOON HW, WHIPP SC, ARGENZIO RA, LEVINE MM, GIANNELLA RA. Attaching and effacing activities of rabbit and human enteropathogenic *Escherichia coli* in pig and rabbit intestines. *Infect. Immun*. 1983; 41:1340–1351. [PubMed: 6350186]
- MUNDY R, PETROVSKA L, SMOLLETT K, SIMPSON N, WILSON RK, YU J, TU X, ROSENSHINE I, CLARE S, DOUGAN G, FRANKEL G. Identification of a novel *Citrobacter rodentium* type III secreted protein, EspI, and roles of this and other secreted proteins in infection. *Infection and immunity*. 2004; 72:2288–302. [PubMed: 15039354]
- NAGANO K, TAGUCHI K, HARA T, YOKOYAMA S, KAWADA K, MORI H. Adhesion and colonization of enterohemorrhagic *Escherichia coli* O157:H7 in cecum of mice. *Microbiology and immunology*. 2003; 47:125–32. [PubMed: 12680715]
- NAKAO H, TAKEDA T. *Escherichia coli* Shiga toxin. *Journal of natural toxins*. 2000; 9:299–313. [PubMed: 10994531]
- NART P, NAYLOR SW, HUNTLEY JF, MCKENDRICK II, GALLY DL, LOW JC. Responses of cattle to gastrointestinal colonization by *Escherichia coli* O157:H7. *Infection and immunity*. 2008; 76:5366–72. [PubMed: 18765741]
- NOUGAYREDE JP, FERNANDES PJ, DONNENBERG MS. Adhesion of enteropathogenic *Escherichia coli* to host cells. *Cell Microbiol*. 2003; 5:359–72. [PubMed: 12780774]
- OBRIG TG. *Escherichia coli* Shiga Toxin Mechanisms of Action in Renal Disease. *Toxins (Basel)*. 2010; 2:2769–2794. [PubMed: 21297888]
- OGURA Y, OOKA T, WHALE A, GARMENDIA J, BEUTIN L, TENNANT S, KRAUSE G, MORABITO S, CHINEN I, TOBE T, ABE H, TOZZOLI R, CAPRIOLI A, RIVAS M, ROBINS-BROWNE R, HAYASHI T, FRANKEL G. TccP2 of O157:H7 and non-O157 enterohemorrhagic *Escherichia coli* (EHEC): challenging the dogma of EHEC-induced actin polymerization. *Infection and immunity*. 2007; 75:604–12. [PubMed: 17101643]
- PENNINGTON H. *Escherichia coli* O157. *Lancet*. 2010; 376:1428–35. [PubMed: 20971366]
- PERALTA-RAMIREZ J, HERNANDEZ JM, MANNING-CELA R, LUNA-MUNOZ J, GARCIA-TOVAR C, NOUGAYREDE JP, OSWALD E, NAVARRO-GARCIA F. EspF Interacts with

nucleation-promoting factors to recruit junctional proteins into pedestals for pedestal maturation and disruption of paracellular permeability. *Infect Immun.* 2008; 76:3854–68. [PubMed: 18559425]

- PHILLIPS N, HAYWARD RD, KORONAKIS V. Phosphorylation of the enteropathogenic *E. coli* receptor by the Src-family kinase c-Fyn triggers actin pedestal formation. *Nat Cell Biol.* 2004; 6:618–25. [PubMed: 15220932]
- PIERARD D, DE GREVE H, HAESEBROUCK F, MAINIL J. O157:H7 and O104:H4 Vero/Shiga toxin-producing *Escherichia coli* outbreaks: respective role of cattle and humans. *Veterinary research.* 2012; 43:13. [PubMed: 22330148]
- PSOTKA MA, OBATA F, KOLLING GL, GROSS LK, SALEEM MA, SATCHELL SC, MATHIESON PW, OBRIG TG. Shiga toxin 2 targets the murine renal collecting duct epithelium. *Infect Immun.* 2009; 77:959–69. [PubMed: 19124603]
- RASKO DA, WEBSTER DR, SAHL JW, BASHIR A, BOISEN N, SCHEUTZ F, PAXINOS EE, SEBRA R, CHIN CS, ILIOPOULOS D, KLAMMER A, PELUSO P, LEE L, KISLYUK AO, BULLARD J, KASARSKIS A, WANG S, EID J, RANK D, REDMAN JC, STEYERT SR, FRIMODT-MOLLER J, STRUVE C, PETERSEN AM, KROGFELT KA, NATARO JP, SCHATZ EE, WALDOR MK. Origins of the *E. coli* strain causing an outbreak of hemolytic-uremic syndrome in Germany. *The New England journal of medicine.* 2011; 365:709–17. [PubMed: 21793740]
- RITCHIE JM, BRADY MJ, RILEY KN, HO TD, CAMPELLONE KG, HERMAN IM, DONOHUE-ROLFE A, TZIPORI S, WALDOR MK, LEONG JM. EspF_U, a type III-translocated effector of actin assembly, fosters epithelial association and late-stage intestinal colonization by *E. coli* O157:H7. *Cell Microbiol.* 2008; 10:836–47. [PubMed: 18067584]
- RITCHIE JM, THORPE CM, ROGERS AB, WALDOR MK. Critical roles for stx2, eae, and tir in enterohemorrhagic *Escherichia coli*-induced diarrhea and intestinal inflammation in infant rabbits. *Infect Immun.* 2003; 71:7129–39. [PubMed: 14638803]
- RITCHIE JM, WALDOR MK. The locus of enterocyte effacement-encoded effector proteins all promote enterohemorrhagic *Escherichia coli* pathogenicity in infant rabbits. *Infection and immunity.* 2005; 73:1466–74. [PubMed: 15731044]
- RIVERA GM, BRICENO CA, TAKESHIMA F, SNAPPER SB, MAYER BJ. Inducible clustering of membrane-targeted SH3 domains of the adaptor protein Nck triggers localized actin polymerization. *Current biology : CB.* 2004; 14:11–22. [PubMed: 14711409]
- ROBINSON CM, SINCLAIR JF, SMITH MJ, O'BRIEN AD. Shiga toxin of enterohemorrhagic *Escherichia coli* type O157:H7 promotes intestinal colonization. *Proceedings of the National Academy of Sciences of the United States of America.* 2006; 103:9667–72. [PubMed: 16766659]
- ROHATGI R, NOLLAU P, HO HY, KIRSCHNER MW, MAYER BJ. Nck and phosphatidylinositol 4,5-bisphosphate synergistically activate actin polymerization through the N-WASP-Arp2/3 pathway. *The Journal of biological chemistry.* 2001; 276:26448–52. [PubMed: 11340081]
- SANGER JM, CHANG R, ASHTON F, KAPER JB, SANGER JW. Novel form of actin-based motility transports bacteria on the surfaces of infected cells. *Cell Motil Cytoskeleton.* 1996; 34:279–87. [PubMed: 8871815]
- SAUTER KA, MELTON-CELSA AR, LARKIN K, TROXELL ML, O'BRIEN AD, MAGUN BE. Mouse model of hemolytic-uremic syndrome caused by endotoxin-free Shiga toxin 2 (Stx2) and protection from lethal outcome by anti- Stx2 antibody. *Infection and immunity.* 2008; 76:4469–78. [PubMed: 18694970]
- SCHAUER DB, FALKOW S. Attaching and effacing locus of a *Citrobacter freundii* biotype that causes transmissible murine colonic hyperplasia. *Infect Immun.* 1993a; 61:2486–92. [PubMed: 8500884]
- SCHAUER DB, FALKOW S. The eae gene of *Citrobacter freundii* biotype 4280 is necessary for colonization in transmissible murine colonic hyperplasia. *Infect Immun.* 1993b; 61:4654–61. [PubMed: 8406863]
- SCHEIRING J, ANDREOLI SP, ZIMMERHACKL LB. Treatment and outcome of Shiga-toxin-associated hemolytic uremic syndrome (HUS). *Pediatric nephrology.* 2008; 23:1749–60. [PubMed: 18704506]

- SCHMIDT H. Shiga-toxin-converting bacteriophages. *Research in microbiology*. 2001; 152:687–95. [PubMed: 11686382]
- SCHULLER S. Shiga toxin interaction with human intestinal epithelium. *Toxins*. 2011; 3:626–39. [PubMed: 22069729]
- SCHULLER S, CHONG Y, LEWIN J, KENNY B, FRANKEL G, PHILLIPS AD. Tir phosphorylation and Nck/N-WASP recruitment by enteropathogenic and enterohaemorrhagic *Escherichia coli* during ex vivo colonization of human intestinal mucosa is different to cell culture models. *Cell Microbiol*. 2007a; 9:1352–64. [PubMed: 17474908]
- SCHULLER S, HEUSCHKEL R, TORRENTE F, KAPER JB, PHILLIPS AD. Shiga toxin binding in normal and inflamed human intestinal mucosa. *Microbes Infect*. 2007b; 9:35–9. [PubMed: 17208032]
- SHANER NC, SANGER JW, SANGER JM. Actin and alpha-actinin dynamics in the adhesion and motility of EPEC and EHEC on host cells. *Cell Motil Cytoskeleton*. 2005; 60:104–20. [PubMed: 15627283]
- SHERMAN PM, BOEDEKER EC. Regional differences in attachment of enteroadherent *Escherichia coli* strain RDEC-1 to rabbit intestine: luminal colonization but lack of mucosal adherence in jejunal self-filling blind loops. *Journal of pediatric gastroenterology and nutrition*. 1987; 6:439–44. [PubMed: 3323438]
- SIMMONS CP, CLARE S, GHAEM-MAGHAMI M, UREN TK, RANKIN J, HUETT A, GOLDIN R, LEWIS DJ, MACDONALD TT, STRUGNELL RA, FRANKEL G, DOUGAN G. Central role for B lymphocytes and CD4+ T cells in immunity to infection by the attaching and effacing pathogen *Citrobacter rodentium*. *Infection and immunity*. 2003; 71:5077–86. [PubMed: 12933850]
- SNAPPER SB, TAKESHIMA F, ANTON I, LIU CH, THOMAS SM, NGUYEN D, DUDLEY D, FRASER H, PURICH D, LOPEZ-ILASACA M, KLEIN C, DAVIDSON L, BRONSON R, MULLIGAN RC, SOUTHWICK F, GEHA R, GOLDBERG MB, ROSEN FS, HARTWIG JH, ALT FW. N-WASP deficiency reveals distinct pathways for cell surface projections and microbial actin-based motility. *Nat Cell Biol*. 2001; 3:897–904. [PubMed: 11584271]
- SRIKANTH CV, WALL DM, MALDONADO-CONTRERAS A, SHI HN, ZHOU D, DEMMA Z, MUMY KL, MCCORMICK BA. Salmonella pathogenesis and processing of secreted effectors by caspase-3. *Science*. 2010; 330:390–3. [PubMed: 20947770]
- SWIMM A, BOMMARIUS B, LI Y, CHENG D, REEVES P, SHERMAN M, VEACH D, BORNMANN W, KALMAN D. Enteropathogenic *E. coli* Use Redundant Tyrosine Kinases to Form Actin Pedestals. *Mol Biol Cell*. 2004
- TARR PI, GORDON CA, CHANDLER WL. Shiga-toxin-producing *Escherichia coli* and haemolytic uraemic syndrome. *Lancet*. 2005; 365:1073–86. [PubMed: 15781103]
- TZIPORI S, GUNZER F, DONNENBERG MS, DE MONTIGNY L, KAPER JB, DONOHUE-ROLFE A. The role of the *eaeA* gene in diarrhea and neurological complications in a gnotobiotic piglet model of enterohemorrhagic *Escherichia coli* infection. *Infection and immunity*. 1995; 63:3621–7. [PubMed: 7642299]
- VALLANCE BA, DENG W, KNODLER LA, FINLAY BB. Mice lacking T and B lymphocytes develop transient colitis and crypt hyperplasia yet suffer impaired bacterial clearance during *Citrobacter rodentium* infection. *Infection and immunity*. 2002; 70:2070–81. [PubMed: 11895973]
- VINGADASSALOM D, CAMPELLONE KG, BRADY MJ, SKEHAN B, BATTLE SE, ROBBINS D, KAPOOR A, HECHT G, SNAPPER SB, LEONG JM. Enterohemorrhagic *E. coli* requires N-WASP for efficient type III translocation but not for EspF_U-mediated actin pedestal formation. *PLoS Pathog*. 2010; 6
- VLISIDOU I, DZIVA F, LA RAGIONE RM, BEST A, GARMENDIA J, HAWES P, MONAGHAN P, CAWTHRAW SA, FRANKEL G, WOODWARD MJ, STEVENS MP. Role of intimin-tir interactions and the tir-cytoskeleton coupling protein in the colonization of calves and lambs by *Escherichia coli* O157:H7. *Infect Immun*. 2006; 74:758–64. [PubMed: 16369035]
- WALES AD, PEARSON GR, SKUSE AM, ROE JM, HAYES CM, COOKSON AL, WOODWARD MJ. Attaching and effacing lesions caused by *Escherichia coli* O157:H7 in experimentally inoculated neonatal lambs. *Journal of medical microbiology*. 2001; 50:752–8. [PubMed: 11549176]

- WHALE AD, GARMENDIA J, GOMES TA, FRANKEL G. A novel category of enteropathogenic *Escherichia coli* simultaneously utilizes the Nck and TccP pathways to induce actin remodelling. *Cell Microbiol.* 2006; 8:999–1008. [PubMed: 16681840]
- WHITEHEAD RH, ROBINSON PS. Establishment of conditionally immortalized epithelial cell lines from the intestinal tissue of adult normal and transgenic mice. *American journal of physiology. Gastrointestinal and liver physiology.* 2009; 296:G455–60. [PubMed: 19109407]
- WILES S, CLARE S, HARKER J, HUETT A, YOUNG D, DOUGAN G, FRANKEL G. Organ specificity, colonization and clearance dynamics *in vivo* following oral challenges with the murine pathogen *Citrobacter rodentium*. *Cell Microbiol.* 2004; 6:963–72. [PubMed: 15339271]

Summary

Enterohemorrhagic *E. coli* (EHEC) colonizes the intestine and causes bloody diarrhea and kidney failure by producing Shiga toxin. Upon binding intestinal cells, EHEC triggers a change in host cell shape, generating actin ‘pedestals’ beneath bound bacteria. To investigate the importance of pedestal formation to disease, we infected genetically engineered mice incapable of supporting pedestal formation by an EHEC-like mouse pathogen, or wild type mice with a mutant of that pathogen incapable of generating pedestals. We found that pedestal formation promotes attachment of bacteria to the intestinal mucosa and vastly increases the severity of Shiga toxin-mediated disease.

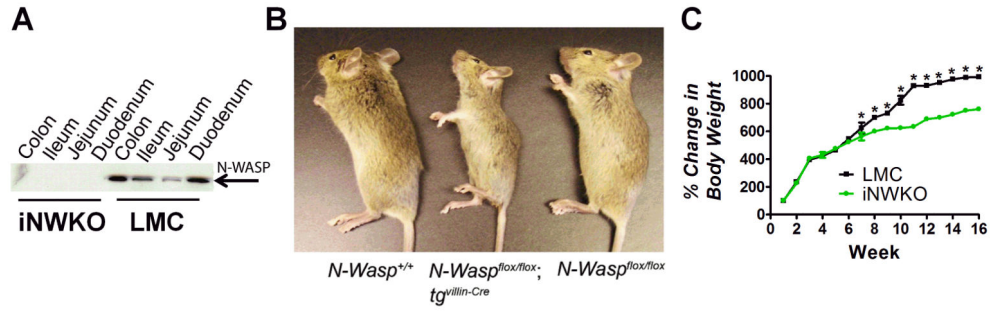


Figure 1. Mice deleted for intestinal N-WASP are viable and fertile but gain less weight than littermate controls

(A) Western blot analysis of N-WASP expression in intestinal tissue from eight week-old iNWKO and littermate control mice confirmed complete deletion of N-WASP throughout the small and large intestine. Tubulin was used as a loading control. (B) Appearance of wild type (*N-Wasp*^{+/+}), iNWKO (*NWasp*^{flox/flox} *tg*^{vil-Cre}), and littermate control (*N-Wasp*^{flox/flox}) mice at twelve weeks. (C) Mean change in body weight over time, ±SEM, of iNWKO and littermate control mice. Data represent five mice per group. Black squares: littermate control mice. Green circles: iNWKO mice. (*): indicates a statistical difference between iNWKO and littermate control mice as determined by two-way ANOVA followed by Bonferroni post-tests (p<0.05).

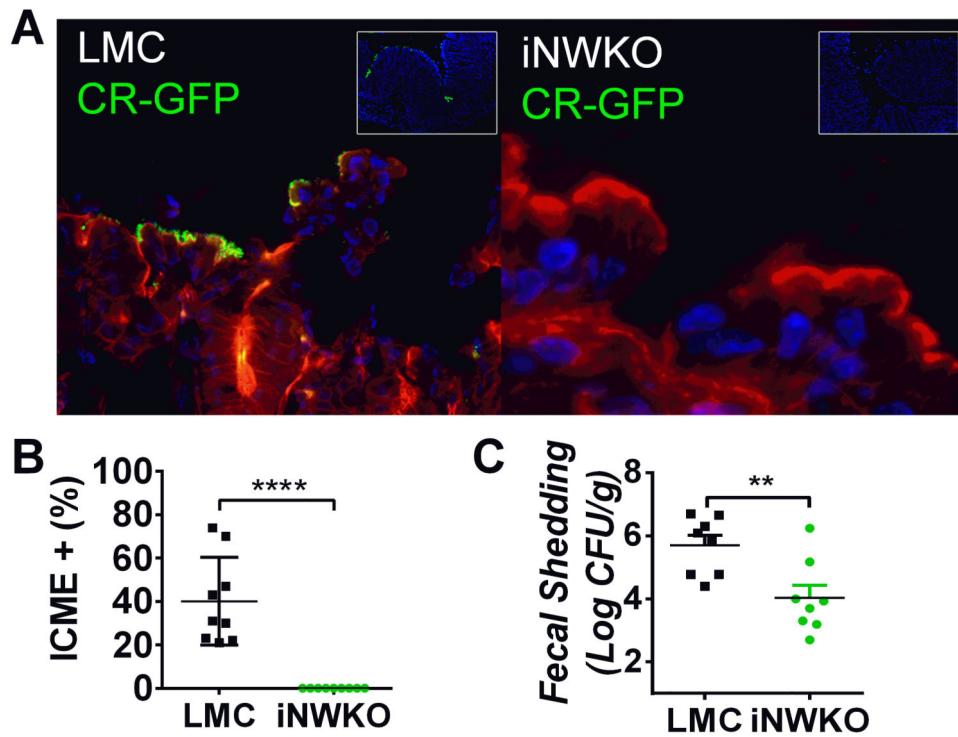


Figure 2. Intestinal N-WASP is required for colonization of mice by *C. rodentium*
 (A) Littermate control and iNWKO mice were infected with 5×10^8 GFP-*C. rodentium* by oral gavage. At four days post-infection, after DAPI-staining (blue) to visualize intestinal cells and phalloidin-staining (red) to visualize the cell architecture, large numbers of adherent GFP-positive *C. rodentium* were identified in littermate control mice (left panel) but not iNWKO mice (right panel). Inset shows low power view of DAPI and GFP, indicating the absence of identifiable *C. rodentium* in iNWKO mice. (B) Intercrypt mucosal epithelium (ICME) with adherent GFP+ *C. rodentium* was quantified in littermate control and iNWKO mice at four days post-infection. Shown is the mean \pm SD. Statistical significance was determined by one-way t-test and ****, $p < 0.0001$. (C) Fecal shedding (\pm SEM) of iNWKO or littermate control mice at seven days post-infection by *C. rodentium* was determined by quantifying viable stool counts. Data reflect a compilation of two experiments, with a total of four mice per group per experiment. (** $p < 0.01$; by an unpaired t-test).

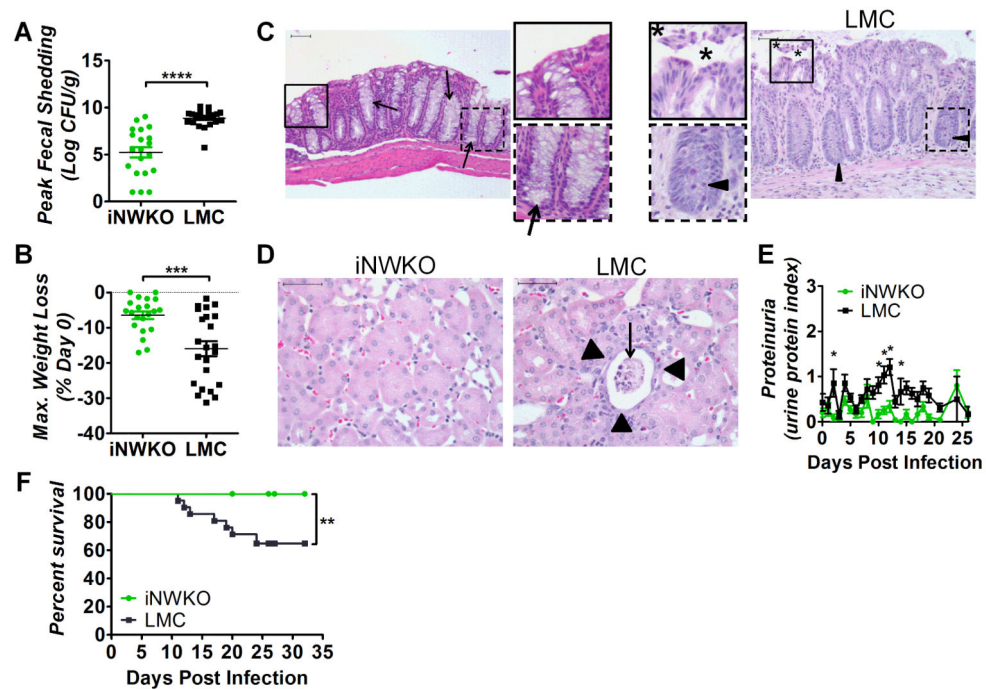


Figure 3. N-WASP promotes high-level colonization and systemic disease during *C. rodentium* (Φ *stx*_{2*dact*}) infection

(A) Fecal shedding by iNWKO or littermate control mice infected with *C. rodentium* (Φ *stx*_{2*dact*}) shown as peak CFU (\pm SEM) of 21 iNWKO and 22 littermate controls from a compilation of five experiments. (****, $p < 0.0001$ by unpaired t-test). (B) Maximum percent body weight loss during infection of iNWKO or littermate control mice infected with *C. rodentium* (Φ *stx*_{2*dact*}) (\pm SEM) of 21 iNWKO and 23 littermate controls from a compilation of five experiments. (***, $p < 0.001$ by unpaired t-test). (C, D) H&E stained intestinal (C) and kidney (D) sections of iNWKO and littermate control mice infected with *C. rodentium* (Φ *stx*_{2*dact*}) at 11 days post-infection. Scale bars measure 50 μ m. Insets: magnification of original images. (C) Asterisks indicate disrupted and sloughed intestinal mucosa. Arrow heads and arrows indicate inflammation and goblet cells, respectively. Magnification, 200x. (D) Arrowheads indicate flattened tubule lining and arrows indicate sloughed tubules and necrotic tissue. Magnification, 400x. (E) Urine protein content, represented as average protein index (\pm SEM), in iNWKO and littermate control mice infected with *C. rodentium* (Φ *stx*_{2*dact*}). Data are a compilation of three experiments, comprising a total of 15 iNWKO and 16 littermate control mice. (*, $p < 0.05$ by repeated measures 2-way ANOVA followed by Bonferroni post-tests; in addition, as described in **Materials and Methods**, the return of average proteinuria toward baseline depicted in the graph preceded clinical recovery of individual mice by a few days). (F) Percent survival of iNWKO and littermate control mice infected with *C. rodentium* (Φ *stx*_{2*dact*}). Data represent a compilation of five experiments, comprising a total of 19 iNWKO mice and 21 littermate controls. Statistical significance was determined using a Log-rank (Mantel-Cox) Test, revealing a significant ($p < 0.01$) difference between the two groups.

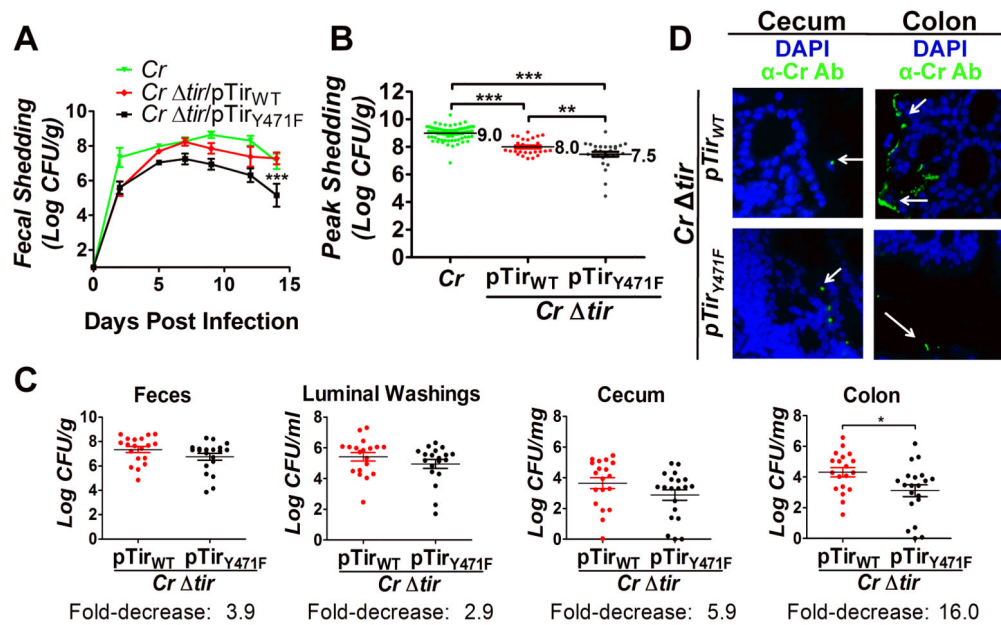


Figure 4. Tir-mediated actin assembly by *C. rodentium* promotes colonization of the colonic mucosa

(A) Fecal shedding by mice infected with the indicated strain was determined. Data represent the mean CFU (\pm SEM) from groups of five mice in one of six experiments. “****” ($p < 0.01$, by repeated measures 2-way ANOVA followed by Bonferroni post-tests) indicates a statistically significant difference from *C. rodentium* or *C. rodentium tir*/pTir_{WT}. (B) Mean peak fecal shedding by mice infected with the indicated strain \pm SEM. Data are a compilation of 14 experiments for wild type *C. rodentium* and five experiments for *C. rodentium tir*/pTir_{WT} or *C. rodentium tir*/pTir_{Y471F}. Each data point represents an individual mouse. Log mean peak fecal shedding is given to the right of each set. (**, $p < 0.01$; ***, $p < 0.001$). (C) Fecal shedding by mice infected with *C. rodentium tir*/pTir_{WT} and *C. rodentium tir*/pTir_{Y471F} at six days post-infection (left panel). Luminal colonization was measured by determining CFU/ml of luminal washings (second panel). Intestinal colonization (cecum and colonic) was measured by determining CFU/mg of tissue homogenate (right two panels). Depicted is a compilation of four individual experiments with three-to-ten mice per group. Each data point represents an individual mouse. Horizontal line indicates the mean, and fold decrease in colonization by *C. rodentium tir*/pTir_{Y471F} compared with *C. rodentium tir*/pTir_{WT} is shown below. Error bars indicate \pm SEM. (*, $p < 0.05$). (D) Cecum and colonic sections of mice infected with the indicated strain were taken at six days post-infection and were stained with DAPI (blue) and anti-*Citrobacter* antibody (green). For these mice, fecal shedding of bacterial strains was equivalent ($1.1 \times 10^7/g$ and $2.8 \times 10^7/g$ for *C. rodentium tir*/pTir_{WT} and *C. rodentium tir*/pTir_{Y471F}, respectively for the cecum sections, and $2.8 \times 10^7/g$ and $1.1 \times 10^7/g$ for *C. rodentium tir*/pTir_{WT} and *C. rodentium tir*/pTir_{Y471F}, respectively for the colon sections). Magnification: 600x. White arrows indicate bacteria.

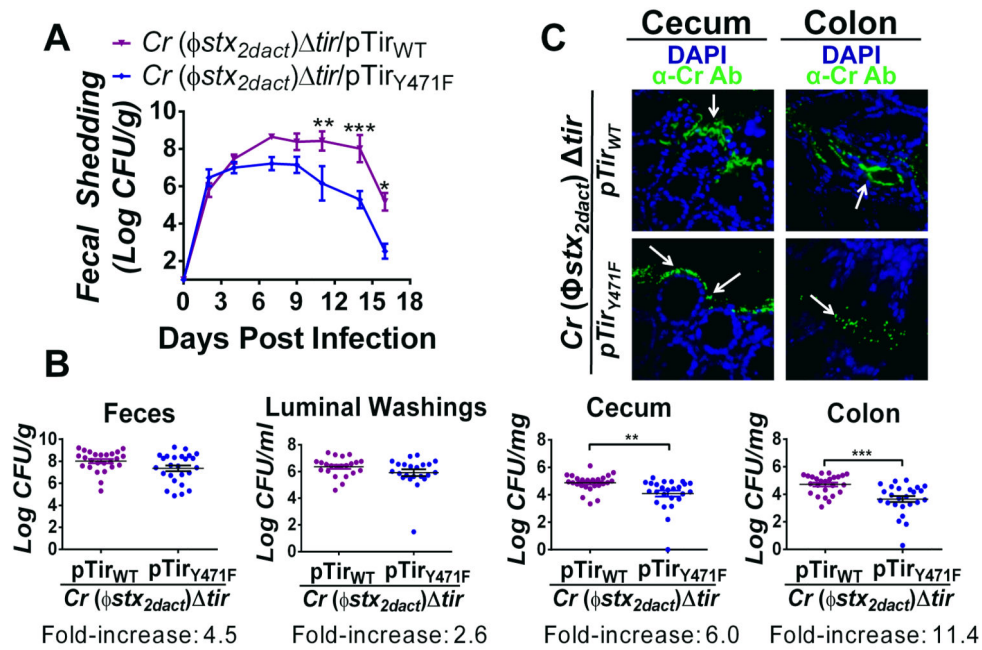


Figure 5. Tir-mediated actin assembly by *C. rodentium* (Φstx_{2dact}) promotes colonization of the colonic mucosa

(A) Fecal shedding by mice infected with the designated strain, represented as the mean CFU (\pm SEM) of groups of five mice. (*, $p < 0.05$; **, $p < 0.01$; and ***, $p < 0.001$; by repeated measures 2-way ANOVA followed by Bonferroni post-tests). Data represent one of five experiments. (B) Fecal shedding by mice infected with *C. rodentium* (Φstx_{2dact}) *tir*/pTir_{WT} and *C. rodentium* (Φstx_{2dact}) *tir*/pTir_{Y471F} at six days post-infection (left panel). Luminal colonization was measured by determining CFU/ml of luminal washings (second panel). Intestinal colonization (cecum and colonic) was measured by determining CFU/mg of tissue homogenate at six days post-infection (right two panels). Data represent a compilation of eight experiments, with three-to-ten mice per group. Each data point represents one mouse. Horizontal line indicates the mean. Fold increase represents the fold change between colonization by *C. rodentium* (Φstx_{2dact}) *tir*/pTir_{WT} and *C. rodentium* (Φstx_{2dact}) *tir*/pTir_{Y471F}. Error bars indicate \pm SEM. (**, $p < 0.01$ and ***, $p < 0.001$). (C) Cecal and colonic sections of mice infected with *C. rodentium* (Φstx_{2dact}) *tir*/pTir_{WT} or *C. rodentium* (Φstx_{2dact}) *tir*/pTir_{Y471F} were taken at ten days post-infection and stained with DAPI (blue) and anti-*Citrobacter* antibody (green). Fecal shedding by each strain was equivalent at both time points. Mice infected with *C. rodentium* (Φstx_{2dact}) *tir*/pTir_{WT} and *C. rodentium* (Φstx_{2dact}) *tir*/pTir_{Y471F} had fecal bacterial loads of 4.8×10^7 /g and 3.6×10^7 /g, respectively. Magnification of IF images is 600x. White arrows indicate bacteria.

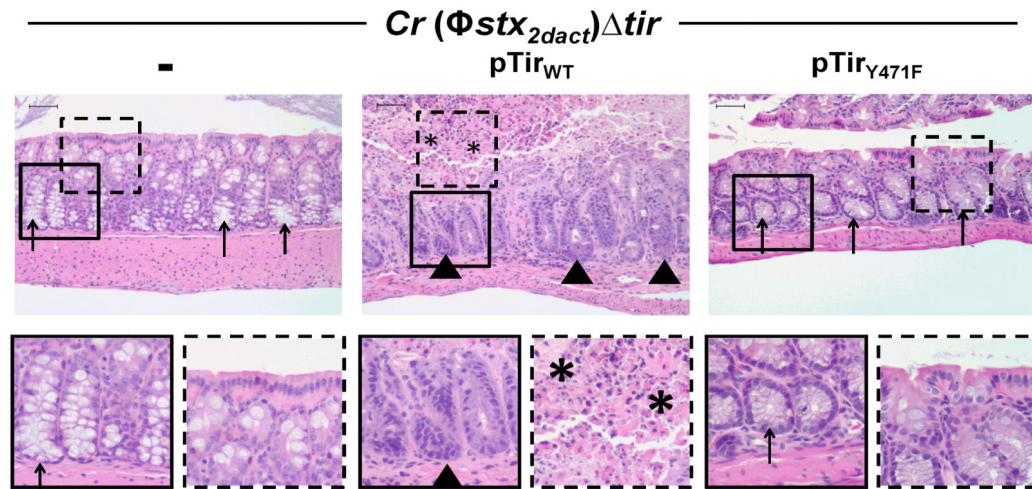


Figure 6. Tir-mediated actin assembly by *C. rodentium* (Φ *stx*_{2*dact*}) promotes intestinal damage
 H&E stained intestinal sections of mice infected with the designated strain, taken at ten days post-infection, are shown at 200x magnification (top row). Bottom row shows a higher magnification of the designated square in the image above. Arrowheads indicate areas of inflammation, arrows indicate areas of goblet cells, and asterisks indicate areas of mucosal surface destruction and necrosis. Scale is 50 μ m.

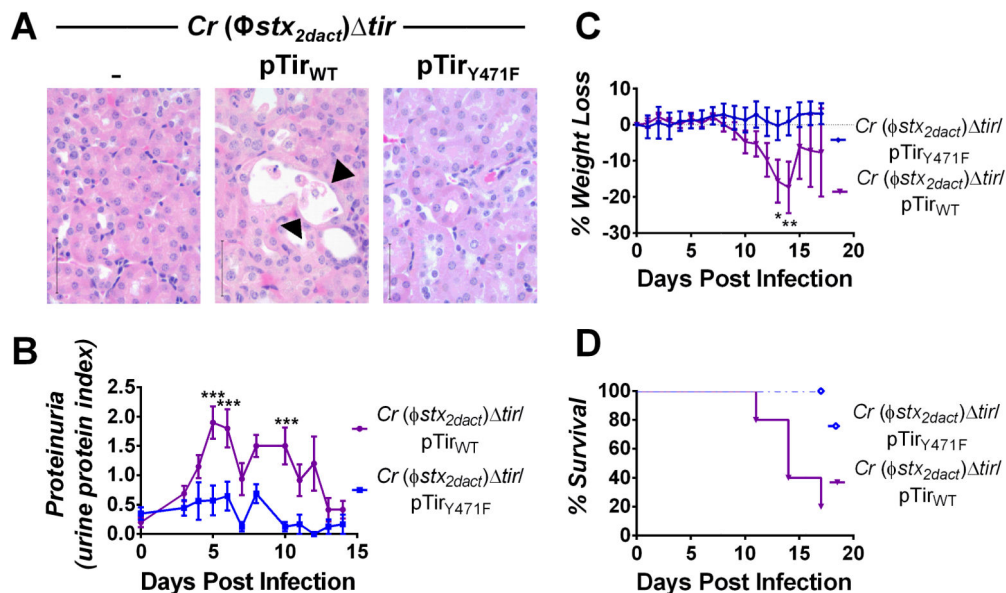


Figure 7. Tir-mediated actin assembly by *C. rodentium* (Φ *stx*_{2dact}) promotes renal damage, weight loss, and death

(A) H&E-stained kidney sections from mice infected with the designated strain, taken at ten days post-infection. Sloughing and attenuation of epithelial cells within the proximal tubules is indicated by arrowheads. Scale bars are 50 μ m, magnification, 600x. (B) Urine protein content in mice infected with the designated strain is represented as mean proteinuria index (\pm SEM), where 0 indicates undetectable protein, 0.5 indicates trace amounts, 1.0 = \sim 30 mg/dl, 2.0 = \sim 100 mg/dl, and 3.0 = \sim 500 mg/dl. Data represent one of two experiments, with five-ten mice per group. (***, $p < 0.001$ by repeated measures 2-way ANOVA followed by Bonferroni post-tests). 6/10 mice infected with *C. rodentium* (Φ *stx*_{2dact}) *tir*/pTir_{WT} developed proteinuria during infection and fully recovered by two weeks post-infection; in addition, as described in **Materials and Methods**, the return of average proteinuria toward baseline depicted in the graph preceded clinical recovery of individual mice by a few days, as described in **Materials and Methods**). (C) Weight loss in mice infected with the designated strain was determined and expressed as percent change from day zero weight. Shown are the means (\pm SEM) of five mice per group. Data represent one of six independent experiments. (*, $p < 0.05$ and **, $p < 0.01$ by repeated measures 2-way ANOVA followed by Bonferroni post-tests; in addition, as described in **Materials and Methods**, the return of average weight toward baseline depicted in the graph preceded clinical recovery of individual mice by a few days). (D) Percent survival of mock-infected mice or mice infected with the designated strain. Data shown represent one of five experiments. Statistical significance was determined using a Log-rank (Mantel-Cox) Test and revealed a significant ($p < 0.05$) difference between the two groups.

Table 1

Enhanced fecal shedding is associated with the ability to generate actin pedestals and with lysogeny by Φ *stx_{2dact}*.

Parental strain	Log peak fecal shedding			Shedding defect of pTir _{Y471F} vs. pTir _{WT} (p value)
	WT	<i>tir</i> /pTir _{WT}	<i>tir</i> /pTir _{Y471F}	
<i>C. rodentium</i>	9.0 (\pm 0.05) (n=82)	8.0 (\pm 0.11) (n=28)	7.5 (\pm 0.17) (n=28)	3.2-fold (p=0.0121)
<i>C. rodentium</i> (Φ <i>stx_{2dact}</i>)	9.8 (\pm 0.04) (n=132)	8.8 (\pm 0.17) (n=39)	8.1 (\pm 0.14) (n=20)	5.0-fold (p=0.0082)
Increase associated with Φ <i>stx_{2dact}</i> (p value)	6.3-fold (p<0.0001)	6.3-fold (p=0.0008)	4.0-fold (p=0.0172)	

¹ n = number indicates the number of mice infected with the designated strain, and is a compilation of results from four or more experiments.

² p = p value by two-tailed, unpaired Student's t-test.

Table 2

The ability to generate actin pedestals is associated with colonization of the colonic mucosa.

Strain harboring plasmid	% positive cecal samples ¹		% positive colonic samples	
	pTir _{WT}	pTir _{Y471F}	pTir _{WT}	pTir _{Y471F}
<i>C. rodentium</i> <i>tir</i>	53% (9/17) ²	12%* (2/17)	53% (9/17)	0%* (0/17)
<i>C. rodentium</i> <i>tir</i> (Φ stx2 _{lact})	72% (13/18)	26%* [†] (5/19)	72% (13/18)	0%* (0/19)

¹ Intestinal samples with bacteria adherent to the epithelium were scored positive (see **Materials and Methods**).

² Denotes the number of mice with samples positive for mucosally adherent bacteria divided by the total number of mice analyzed.

* The percentage of positive samples was significantly ($p < 0.05$ by Student's t-test) less than that found for the isogenic strain producing wild type Tir infecting the corresponding intestinal segment.

[†] The percentage of positive cecal samples was significantly ($p < 0.05$ by Student's t-test) greater than that found for the identical strain infecting the colon.

Table 3

Actin pedestal formation promotes lethal infection.

Range of fecal shedding (log)	<i>Cr</i> (Φ <i>stx</i> _{2<i>dact</i>}) <i>tir</i> /p <i>Tir</i> _{WT}		<i>Cr</i> (Φ <i>stx</i> _{2<i>dact</i>}) <i>tir</i> /p <i>Tir</i> _{Y471F}	
	Average log fecal shedding	% Lethality (# dead/total)	Average log fecal shedding	% Lethality (# dead/total)
9.7-10.7	9.8	80% (4/5)	na	na
9.1-9.7	9.3	91% (10/11)	9.4	100% (1/1)
8.3-9.1	8.8	53% (8/15)	8.8	0%* (0/5)
7.7-8.3	8.0	60% (3/5)	8.0	0%* (0/8)
<u>Below 7.7</u>	<u>4.8</u>	<u>0%</u> (0/4)	<u>7.4</u>	<u>0%</u> (0/6)
Total	8.8	62.5% (25/40)	8.1	5% (1/20)

* statistically significant defect in lethality compared to mice infected with *C. rodentium* (Φ *stx*_{2*dact*}) *tir*/p*Tir*_{WT} (p<0.05).

na, not applicable.